

# 國立交通大學

電子工程學系 電子研究所碩士班

## 碩士論文

奈米線薄膜電晶體於生化感測應用之研究

**Study of Nanowires Thin-Film-Transistor  
for Biochemical Sensor applications**

研究生：王子銘

指導教授：林鴻志 博士

柯富祥 博士

黃調元 博士

中華民國九十六年六月

奈米線薄膜電晶體於生化感測應用之研究

Study of Nanowires Thin-Film-Transistor  
for Biochemical Sensor applications

研究生：王子銘

Student：Tzu-Ming Wang

指導教授：林鴻志 博士

Advisors：Dr. Horng-Chih Lin

柯富祥 博士

Dr. Fu-Hsiang Ko

黃調元 博士

Dr. Tiao-Yuan Huang



國立交通大學  
電子工程學系 電子研究所碩士班  
碩士論文

A Thesis

Submitted to Department of Electronics Engineering & Institute of Electronics

College of Electrical Engineering and Computer Science

National Chiao-Tung University

in Partial Fulfillment of the Requirements

for the Degree of

Master of Science

in

Electronic Engineering

June 2007

Hsinchu, Taiwan, Republic of China

中華民國九十六年六月

# 國立交通大學

## 論文口試委員會審定書

本校 電子工程學系 電子研究所 王子銘 君

所提論文：奈米線薄膜電晶體於生化感測應用之研究

合於碩士資格標準，業經本委員會評審認可。

口試委員：林鴻志 黃調元  
林鴻志 黃調元

柯富祥 楊裕雄  
柯富祥 楊裕雄

指導教授：林鴻志 柯富祥  
林鴻志 柯富祥

所 長：邱碧秀

系 主 任：周世傑  
周世傑

中華民國 96 年 6 月 27 日

# 奈米線薄膜電晶體於生化感測應用之研究

研究生：王子銘

指導教授：林鴻志博士

柯富祥博士

黃調元博士

國立交通大學

電子工程學系

電子研究所

## 摘要

一維的各種奈米材料,例如奈米探管和奈米線...由於他們特別的電、光、和機械特性,近年來吸引了大家的目光,而被廣泛的研究著。

在本論文中,我們成功使用一種簡單而快速的方法製備出各種不同特性的奈米線電晶體,並且利用他高靈敏的特性與微流道系統做結合,在不同的環境中,奈升等級的待測液體由幫浦注射,透過微流道控制通過奈米線表面,希望能利用不同領域的優點之結合在生化感測方面有所突破。

我們利用側壁形成奈米線,且研究探討各種改良方法如摻雜,多通道,及不一樣環境對電性的影響,並成功偵測蛋白質吸附之變化,吸附在奈米線表面的不同電荷改變了電晶體的各種電性,也提供了實驗室晶片應用的一個新方向。

# Study of Nanowires Thin-Film-Transistor for Biochemical Sensor applications

Student: Tzu-Ming Wang

Adviser: Dr. Horng-Chih Lin

Dr. Fu-Hsiang Ko

Dr. Tiao-Yuan Huang

Department of Electronics Engineering & Institute of Electronics

National Chiao Tung University



Abstract:

One-dimensional (1D) nanomaterials, such as nanotubes and nanowires, recently have drawn a great deal of attention due to their extraordinary optical, mechanical, and electrical properties ◦

In this thesis, we fabricate and integrate high sensitivity nanowires field effect transistor and Microfluidic system successfully. The microfluidic channel provides control over reagent flow and different sample. We hope that the advantages of different fields can breakthrough in biochemical sensing area.

The electrical characteristic of different channel doping, multiple channels devices were also investigated. They charged molecules adsorbed onto the nanowire

channel and modified the electronic property. The novel combination provide a way for future lab-on-a-chip applications.



## Acknowledgement

兩年很快就過去了,很開心終於完成了這本碩士論文,裡面記錄了兩年來實驗的小小成果,在這過程感謝林鴻志和黃調元博士的指導和要求,不論在生活中或課業研究上都學習到許多,還有謝謝柯富祥博士在研究上觀念和方法的教導並熱心提供儀器,因為你們讓我更加成長,學到很多,對以後進入社會工作受益很大.

感謝帶我作實驗的蘇俊榮學長,不管是製程,量測和分析上都給我很大的幫助,剛好可給我這散散的個性一個督促,還有謝謝呂嘉裕,盧景森,李明賢,徐行徽,張凱翔,在實驗中對我的幫忙和討論,蔡銑泓和黃建銘學長帶我做實驗,討論棒球,洪振家,謝雨霖,趙志誠,呂建松學長和我一起度過歡樂的碩一,我會記得這段美好的時光,也很高興認識一群一起努力的同學,王偉銘,黃建富,蔡子儀,黃育峰,詹凱翔,李克慧,朱馥鈺,林欣逸,萬嘉塵,另外就是李振欽和李振銘,很高興大家一路互相幫忙,學習,希望友誼長存,再來是實驗室的學弟妹洪政雄,陳威臣,李冠彰,林漢仲,江忠祐,洪文強,劉大偉,陳玲,很高興認識你們,讓我留下快樂的回憶.

另外謝謝一路教導鼓勵我的機械所劉懋勳學長還有奈米所的吳佳典學長,幫忙我的夏德玲,吳中書,還有吳亦穠,林志杰,游群芳,黃美榕,蔡依臻,生科所的蕭承允學長,顯示所的梁芸嘉,還有幫我打氣的珮綺,

虹翔,依羚,玫瑰,翊暄,曉瑜,文賢,宜芳,力瑋,加樺和皓皓.

謝謝一路支持我的凱晴,最後感謝我的爸媽對我從小的栽培,還有對我期望很大的妹妹,完成學業要感謝的人太多,還有很多沒提到的人,都在我心中都很重要,謝謝你們,謝謝.

子銘

誌于風城交大 2007/06





# Contents

	Page
Abstract (in Chinese).....	i
Abstract (in English).....	ii
Acknowledgement (in Chinese).....	iv
Contents.....	vi
Tables Captions.....	viii
Figures Captions.....	viii
Chapter 1: Introduction.....	1
1.1 Background.....	1
1.2 Motivation.....	4
1.3 Thesis organization.....	5
Chapter 2: Microfluid System: Fabrication and Integration.....	6
2.1 Microfluidics development and challenges.....	6
2.2 Fabrication and integration of microfluidic channel.....	8
2.3 Physics of microfluidics and semiconductor liquid interface.....	11
Chapter 3: Fabrication and Electrical Characterization of Nanowire Transistors. .....	14
3.1 Device fabrication and measurement setup.....	14
3.2 Measurement results and discussion.....	16
3.3 Engineering of channel doping.....	17

**3.4 Thin-film-transistor with multiple NW-channels.....20**

**3.5 Effect of O<sub>2</sub> plasma treatment and water environment on device  
performance.....21**

**3.6 Nanowire surface modification and biotin-streptavidin sensing.....23**

**Chapter 4: Conclusion.....26**

**4.1 Conclusion.....26**

**4.2 Future work.....27**

**References.....28**



## Tables Captions

	page
Table.1-1: Comparisons of the advantage to other current researches....	37
Table. 2-1: advantages of PDMS for microfluid system.....	38
Table.2-2: $\Theta$ vs. oxygen plasma time.....	38
Table.3-1: threshold voltage for different channel length FET.....	39
Table.3-2: threshold voltage for different channel doping concentration.	39



## Figure Captions

	page
Figure.1-1 Nano cantilevers: absorption of analyte molecules leads to a shift in resonance frequency.....	40
Figure.1-2: Basic components of an instrument for SPR biosensing: a variation in reflectivity of the incident light versus angle or wavelength is proportional to the amount of biopolymer bound near the surface.....	40
Figure.1-3: Sensing operation of ISFET: the amount of charge of the target species bound to the surface determines the drain current of the device.....	41
Figure.1-4: FET with nanowires channels proposed by ADTL lab, NCTU.....	41
Figure.2-1: Size comparison of various engineering and biological components.[Adapted from A. van den Berg].....	42
Figure.2-2: Structural formula of PDMS.....	42
Figure.2-3: SU8 patterns on 4” wafer, Channel length: 3cm; width: 500,or 800um; height of resist thickness is about	

50um.....	43
Figure.2-4: Different design patterns of microfluidics with glass mask..	43
Figure.2-5: Cycle of PDMS microfluid channel.....	44
Figure.2-6: Finished products with in/out tubes.....	45
Figure.2-7: O <sub>2</sub> plasma treatment chamber.....	45
Figure.2-8: Contact angle ( $\Theta$ ) of three materials with O <sub>2</sub> plasma treatment Time.....	46
Figure.2-9: Contact angle measurement system.....	46
Figure.2-10: Surface state of water drop.....	47
Figure.2-11: Combining process of PDMS and nanowire device.....	48
Figure.2-12: Controllable syringe pump.....	49
Figure.2-13: NWs TFT integrated with microfluidic system.....	49
Figure.2-14: Liquid and nanowire interface .....	50
Figure.3-1: Process flow of nanowires poly-Si TFTs.....	51
Figure.3-2: Schematic diagram of sidewall twin Nanowires FET proce.	52
Figure.3-3: Optical microscope image of NWs FET device.....	53
Figure.3-4: SEM graph of sidewall twin nanowires with 47 nm channel width.....	53
Figure.3-5: I <sub>D</sub> -V <sub>GS</sub> transfer characteristics of channel doping P <sub>31+</sub> with	

5 $\mu$ m channel Length.....	54
Figure.3-6: Band diagrams of different gate voltage conditions from depletion(I) to accumulation(III) for N-type device.....	54
Figure.3-7: Transfer characteristics of N/P type NWs-TFT with different channel length.....	56
Figure.3-8: $I_D$ - $V_{GS}$ transfer characteristics of 5 $\mu$ m channel length device with different doping concentration.....	56
Figure.3-9: Plot show the increase of on-current with decreasing channel length for different channel doping level.....	57
Figure3-10: SEM top view picture of 20 multi parallel nanowires channel TFT width $W \sim 40$ nm; channel length $L = 5 \mu$ m.....	57
Figure.3-11: Transfer characteristics of NWs-TFT with different channel number.....	58
Figure.3-12: ISE-TCAD simulation with bottom gate 5V.....	58
Figure.3-13: The $I_D$ - $V_{GS}$ characteristics of different length NWs-TFT with/without oxygen plasma treatment.....	59
Figure.3-14: Transfer characteristic of device working in the air and water.....	59

Figure.3-15: Surface bonds of APTES-modified nanowire  
channel.....60

Figure.3-16: Reaction of NHS -Biotin with a primary amine.  
(source: Avidin-Biotin Chemistry: A Handbook).....60

Figure.3-17: Transfer characteristics of NWs-TFT before and after Biotin  
linking, and sensing of Biotin-Streptavidin.....61



# Chapter 1: Introduction

## 1.1 Background

Metal-oxide-semiconductor field effect transistors (MOSFET) have been investigated as sensors since 1975 by Lundstrom et al, who reported a hydrogen-sensitive MOSFET with palladium as the gate metal (GASFET) [1]. To this date for bio-sensing application, the most common detection method is fluorescent labeling which is complicated and costly in sample preparation, and not available for real-time detection. In addition, tagged molecules problems like non-uniform labeling and signal quenching are observed. Since then a number of label-free approaches, such as nano cantilevers [2], surface plasmon resonance (SPR) [3] and ion sensitive field effect transistors (ISFET) [4], have also been proposed and developed with the intention to overcome the issues stated above.

Micro-electro-mechanical systems (MEMS) built with nano-fabrication technology are used in a variety of sensor applications. One example is the nano cantilevers, as shown in Fig.1-1, which can be used as biological sensors. In this scheme, the adsorption of target species causes a change in mass or surface tension of the cantilever. This leads to the variation in the oscillation amplitude of the cantilever



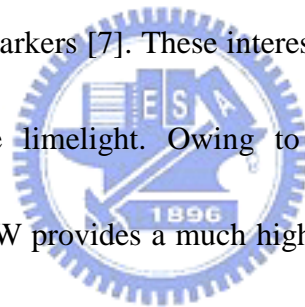
which can be then measured and recorded. The bending can be detected by the deflection of an optical beam or by a change of electrical resistance in a piezoelectric thin film on the cantilever. The smaller the device, the more sensitive to mass change since the resonance frequency is dependant on the total mass .But mass measurement works best in a vacuum. When the sensing is performed in an aqueous solution, the liquid surrounding the oscillator tends to resist the oscillation which in turn may reduce the sensitivity of the measurement.

Figure1-2 shows the configuration of SPR method, in which biomolecules are immobilized on gold-coated glass slide. When light is shined through the glass slide onto the gold surface at angles and wavelengths near the surface plasmon resonance condition, the refractive index and optical reflectivity change very sensitively with the presence of biomolecules attached on the gold surface. The binding is easily observed and quantified by monitoring the change in reflectivity. However, such scheme needs complicated optical system to accomplish and does not have sufficient multiplexing capabilities in its current configuration.

The ISFET is an MOSFET with the gate in the form of a reference electrode inserted in an aqueous solution which is in contact with the gate oxide, as shown in Fig.1-3. Ion groups change the interfacial potential at the solution/oxide interface. This scheme is relatively easy as compared with other approaches, but suffers from

low sensitivity due to the bulk leakage conducted in the substrate. To address this issue, semi-conducting nanotubes or nanowires are good candidate channel materials for the construction of such bio-sensing devices.

Using silicon nanowires as a biosensor were first demonstrated by Lieber and co-workers in 2001 [5]. In addition to sensors, many related studies have been carried out to explore possible applications to nanoelectronics like functioning logic elements and memories. In Lieber's work, vapor-liquid-solid (VLS) was used to prepare nanowires. They showed that the materials are capable of detecting single viruses [6] and identification of cancer markers [7]. These interesting and exciting results put the nanowire bio-sensors in the limelight. Owing to the inherent feature of high surface-to-volume ratio, Si NW provides a much higher sensitivity than conventional planar MOS sensing structure.



However, most of the current experimental works on Si NW devices have been conducted using the bottom-up approach, such as VLS(see appendix), which often exhibits difficulties in controlling the doping level, the shape and critical dimensions accurately. Additional metallic source/drain process is commonly used and a Schottky barrier formed at the metal/semiconductor interface may affect the value and uniformity of the contact resistance. Other disadvantages of bottom-up methods include the difficulty of directly growing highly ordered density arrays and the need

of complicated fabrication flow to construct available device structures.

Top-down schemes represent an alternative approach to address those issues associated with bottom-up approach. Many people applied direct writing e-beam lithography (EBL) and plasma etching techniques to generate NW structures on SOI wafers. The main drawback of EBL is its low throughput.

## 1.2 Motivation

As mentioned above, to make use of NWs as a sensing element requires tight control over a number of parameters, such as the dimensions of the NW structures, relative positioning and alignment of different NWs, and formation of good contacts.

To meet these concerns, recently we have developed a novel method adopting sidewall spacer method to form NWs TFT. The structure is shown in Fig.1-4 [8].  $\text{NH}_3$  plasma passivation, RTA, and MILC method have been investigated and implemented to improve the electrical performance of the fabricated devices. This scheme also represents a potential and promising route for sensing device fabrication. A comparison with previously reported methods is given in Table.1-1.

For practical chemical and biological sensing applications, the testing needs to be proceeded in an aqueous solution. This usually needs a microfluid system to carry out.

In addition, the threshold voltage ( $V_{th}$ ) of the devices should be adjustable and set to a value with good sensitivity. For these reasons, in this work we investigate the related process to build the microfluid testing environment. In addition, ion implantation is employed to adjust the  $V_{th}$ . Our intentions are to develop the necessary skills and to utilize them for the construction of practical bio-sensing systems.

### **1.3 Thesis organization**

This thesis is divided into four chapters. After introducing the background and motivations of this study, in Chapter 2 the fabrication of microfluid channel and how it is integrated with NWS devices are described. In Chapter 3, details for device fabrication and the implant conditions for  $V_{th}$  adjustment are stated. Results of electrical characterization are subsequently given and discussed. Special attention is paid to the  $V_{th}$  adjustment using ion implant technique. Finally, in Chapter 4 a summary of important achievements of this study is given.

# Chapter 2:

## Microfluid System: Fabrication and Integration

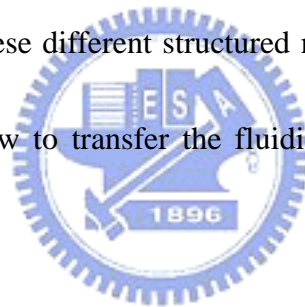
### 2.1 Microfluidics development and challenges

Microfluidics, which studies the motion of fluid and particles through microchannels, is an emerging field that has given rise to a large number of scientific and technological developments over the last few years. There are growing interests to explore microfluidic circuits for chemical reactions and biological operations. In contrast to conventional bench-top setups, microfluidics has been utilized to manipulate processes at microliter ( $\mu\text{L}$ ) to nanoliter (nL) scale (Figure 2-1), such as reduced consumption of reagents (molecular species can be detected on low cells level in an early phase) and improved control over mass and heat transfer. Particularly, miniature analytic systems, the so called lab-on-a-chip systems, have become very popular.

Construction and design of microfluidic devices differ from macro-scale devices. It is not a simple matter to scale conventional devices down straightforwardly, since the dominant physical quantities and properties change in the micro-world. For examples, in the micro world, the liquid flow tends to be laminar, and surface forces

and surface tension start to dominate, while these effects are not significant in the macro scale [9].

Microfabrication technologies have opened up a new research area. Apart from the gain in cost terms, it has become more versatile by opening up to polymers, and the process is also becoming more flexible due to their thermoplastic properties. Polymer molding techniques (e.g., casting of PDMS, PMMA...etc) have been developed for manufacturing of simple fluidic network, but integration into a complete microsystem is far from trivial. At the moment, there are still challenges ahead as to how to couple these different structured microfluidic parts together, how to integrate a sensor, and how to transfer the fluidic part into a microsystem with precision.

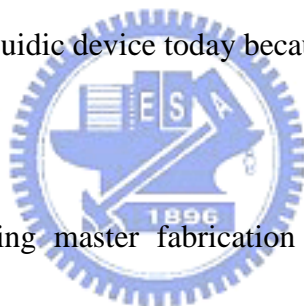


The miniaturized total chemical analysis system ( $\mu$ TAS) concept was first proposed by A Manz and his co-workers [10]. The popularity has been a driving force for the development of new types of microsystems combining electrical and mechanical functions with microfluidic functions, including sample preparation, separation and detection on a small chip.

## 2.2 Fabrication and integration of microfluidic channel

In this section, we will first describe the state-of-the-art technologies used for the manufacturing of microfluidic channel, and then discuss its integration with nanowire sensor device in the second part.

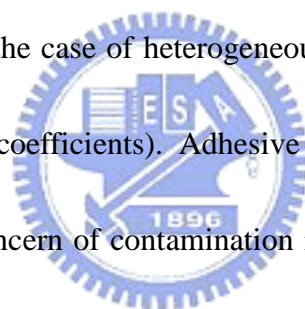
The microchannels were fabricated with replica molding technique which was fabricated by using the Polydimethylsiloxane (PDMS) (Figure 2-2), a process developed by McDonald and Whitesides [11]. PDMS is a clear silicone elastomer from which thin relief fluid channel may be formed easily, and is known to be one of the most attractive materials for microfluidic device today because of its advantageous features shown in Table 2-1.



Two strategies of molding master fabrication have been developed. In one approach, a thick negative photoresist dubbed SU8 is patterned on 4" Si wafer by photolithography. The speed and time of spin coating determine the thickness of the microchannel (typically ~50  $\mu\text{m}$  thick) (Figure 2-3). In the second approach, direct wet etching of the desirable shape (channel region shadowed by chromium) with glass mask by HF is implemented (Figure 2-4). Next, the two prepolymer components of polydimethylsiloxane (Sylgard 184), part A and part B, are mixed together in a 10:1 ratio of part A / part B (this ratio may be modified to yield harder or softer PDMS) and then degassed under vacuum, poured onto the mold and cured for 15min at 80°C in

the oven. After cooling, the cured PDMS is peeled from the mold carefully and rinsed with ethanol because surface cleanness may also play a crucial role in bonding process. Inlet and outlet tubes are inserted. A typical fabrication process of the PDMS microfluid channel is illustrated in Figure 2-5. A finished product is exhibited in Figure 2-6.

An assembly step between two substrates is usually necessary to close the structures. Several types of bonding techniques, such as thermal bonding and anodic bonding, have been developed for different applications. One of the main concerns is the thermal stress, mainly in the case of heterogeneous assembly (i.e., materials with different thermal expansion coefficients). Adhesive bonding is a low temperature process but introduces the concern of contamination into the structure which may be undesirable in microfluidic system.



The PDMS channel sealing does not need any elaborate bonding processes except oxygen plasma treatment so that chemical linking will permanently bind the binding surfaces of the two structures together. The clear PDMS channels are used to seal NW devices after exposing to oxygen plasma (200mTorr, 17W, 30S) (Figure 2-7). A critical issue in the process is that we must align and bond them together immediately after exiting the plasma without unnecessary delay. This is because the surface of oxidized PDMS is known to recover to its original surface condition over



time. In Figs. 2-8~10 and Table 2-2, we show that surface contact angle before and after plasma treatment of silicon, SiO<sub>2</sub> and PDMS. Si–O–Si bonds are created and this assembly becomes irreversible after oxidation of the two parts. How the surface bonds is described in Figure 2-11. A strong bond is important for pumping fluids on chip at high pressure. The detail process sequence is described as follows:

### Bio/nano microfluid System integration

Process Flow:

- 1) Mixing PDMS (20grams): cure agent=10:1 with stirring rod for 5min
- 2) Use vacuum pump to degas about 20min until most bubbles are gone
- 3) Pour it to mother mode (wafer or glass)
- 4) Cure PDMS at 80°C 18min
- 5) Carefully peel off the PDMS structure
- 6) Punch input and output holes
- 7) Surfaces may need to be cleaned with ethanol/IPA
- 8) Surface treatment: O<sub>2</sub> plasma treatment (Pressure=0.2Torr, RF power 17W, time=60s) for both nanowire FET devices and PDMS
- 9) Bond PDMS microfluid system to nanowire devices
- 10) Bake with oven at 90°C for 30min

- 11) Align and press them together
- 12) Insert Teflon tubes to inject sample with string pump (Figure 2-12)
- 13) Test and measure completed samples (Fig. 2-13)

## 2.3: Physics of microfluidics and semiconductor liquid interface

Fundamental understanding of liquid flow through microchannel is important for the design and operation of lab-on-a-chip devices. The classical method of quantifying the turbulent nature of a fluid flow is through examination of the Reynolds number, which gives the ratio of inertial force to viscous force:

$$\text{Re} = \frac{\rho V L_c}{\mu} \quad (\text{Equation 2-1})$$

where  $\rho$  is the density of fluid,  $\mu$  the viscosity of fluid,  $L_c$  the length of channel, and  $V$  the velocity scale of channel

With our experimental conditions, the number can be calculated and the result is

$$\text{Re} = \frac{1\text{g/cm}^3 \times 0.01\text{cm/sec} \times 3\text{cm}}{0.01\text{g/cmsec}} = 3$$

It is commonly accepted that the transition from laminar to turbulent flow occurs at  $Re$  of around 2300. In small microfluid, it is usually lower than 2300, which is representative of laminar flow and difficult for turbulent mixing. This means that the detected sample is focused in low velocity region which maintains minimal impact to nanowire surface which provides an efficient delivery and surface reaction for sensor applications.

A biosensor is based on binding interactions between the immobilised biomolecules and the analyte of interest. The interface between semiconductors and the liquid environment will become increasingly important to understand. When a semiconductor is brought into contact with a solution, electrons can be exchanged between the semiconductor and the solution, and charge flows across the interface until the thermodynamic equilibrium is established.

The applied potential is partitioned between the space charge layer in the semiconductor and the Helmholtz layer on the solution side of the interface (Figure 2-14).

The total potential drop across the interface  $\Delta\Phi_{\text{total}}$  is given by

$$\Delta\Phi_{\text{total}} = \Delta\Phi_{\text{sc}} + \Delta\Phi_{\text{H}} \quad [12]$$

where  $\Delta\Phi_{\text{sc}}$  is potential drop across the semiconductor space charge layer and  $\Delta\Phi_{\text{H}}$  is potential drop across the Helmholtz layer.

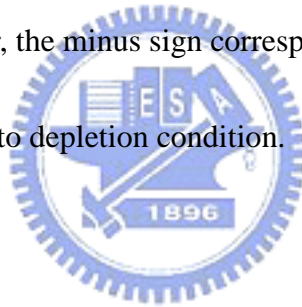
If no charge is trapped in interface states, then

$$Q_{sc} + Q_H = 0$$

The total charge  $Q_{sc}$  is proportional to the electric field at the surface ( $\xi$ ), and can be obtained from Gauss' law and Poisson-Boltzmann equation

$$Q_{sc} = \epsilon \epsilon_0 \xi = (-) (2kT \epsilon \epsilon_0 N_D)^{1/2} (\exp(e \Delta \Phi_{sc} / kT) - (e \Delta \Phi_{sc} / kT) - 1)^{1/2} \quad (\text{Equation 2-2})$$

For n type semiconductor, the minus sign corresponds to accumulation condition, and positive sign corresponds to depletion condition.



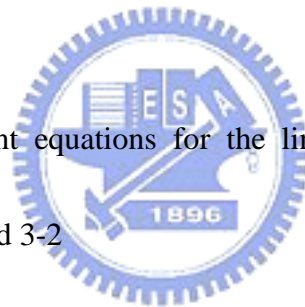
# Chapter 3:

## Fabrication and Electrical Characterization of Nanowire Transistors

### 3.1: Device fabrication and measurement setup

The tested devices in this study were fabricated on 6-inch wafers. First, a tetraethylorthosilicate (TEOS) dummy gate was patterned on Si substrate capped with a wet oxide layer of 1000Å in thickness, followed by the deposition of a low pressure chemical vapor deposition (LPCVD) amorphous silicon film with a thickness of 100nm at 550°C in a furnace tube. Next, light channel implant (p+ for n type, BF<sub>2</sub><sup>+</sup> for p type TFT) was performed. Subsequently, a solid phase crystallization (SPC) annealing step at 600°C for 24hr in N<sub>2</sub> ambient to transform the α-Si to poly-Si, and 30min annealing at 900°C was performed to drive in the dopants. Source/drain(S/D) photoresist patterns were formed by standard lithography step. A transformer coupled plasma (TCP) etching using a gas mixture of Cl<sub>2</sub> and HBr plasma etch step was used to form the sidewall spacer nanowire channel and S/D at the same time. Then, source/drain heavy implant with a dose of 5E15 cm<sup>2</sup> was performed and the dopants

were activated by 30min anneal at 900°C. Finally, a 300nm thick plasma enhanced chemical vapor deposition (PECVD) oxide passivation layer was deposited, the contact and sensing area were opened. The nanowire device fabrication steps are illustrated in Figure 3-1 and Figure 3-2. Figure 3-3 shows the device optical microscope image. The SEM picture of a transistor with channel width=47nm is shown in Figure 3-4. Electrical characteristics were measured with a HP4156 system. All devices were measured with a bottom gate and on a hot chuck with temperature fixed at 298 K.



In this study, the current equations for the linear and saturation regime are expressed in Equations 3-1 and 3-2

Linear region:

$$I_{DS} = (\mu W C_{ox} / L) ((V_{gs} - V_{th}) V_{ds} - V_{ds}^2) \quad (\text{Equation 3-1})$$

Saturation region:

$$I_{DS} = (\mu W C_{ox} / L) ((V_{gs} - V_{th})^2) \quad (\text{Equation 3-2})$$

where  $V_{gs}$  is the gate voltage (volt),  $V_{th}$  is the threshold voltage (volt),  $V_{ds}$  is the drain to source voltage (volts),  $\mu$  is the electron mobility ( $\text{cm}^2/\text{Vs}$ ),  $C_{ox}$  is the gate capacitance ( $\text{F}/\text{cm}^2$ ),  $W$  is the width of the channel (cm),  $L$  is the length of the channel (cm).

The threshold voltage ( $V_{th}$ ) is calculated when

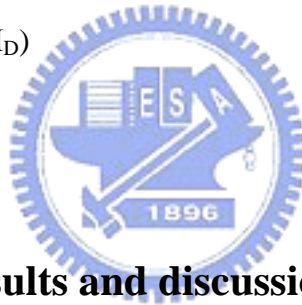
$$I_D = (W/L) 10nA, \text{ at } V_{ds}=0.1, 1V \quad (\text{Equation 3-3})$$

The field effect mobility is determined from transconductance  $g_m$  by

$$\mu_{fe} = L g_m / W C_{OX} V_{DS} \quad (\text{Equation 3-4})$$

Subthreshold swing (SS) could be calculated from subthreshold current by

$$SS = \partial V_G / \partial (\log I_D) \quad (\text{Equation 3-5})$$



### 3.2: Measurement results and discussion

The transfer characteristics of a device with  $L=5\mu m$  and phosphorous ( $5E13cm^{-2}$ ) light channel doping operated in the accumulation mode are shown in Fig. 3-5. Upon application of positive  $V_{GS}$ ,  $I_D$  increases as the majority carrier (electron) density accumulates in the channel. While applying a negative  $V_{GS}$  depletes electrons in the channel and turns the device off.

Family curves are shown when the gate voltage sweeps from  $-5V$  to  $15V$  with  $V_{ds}=0.1/1V$ . The  $I_D-V_{GS}$  curves correspond to three regimes: (I) electron depletion, (II) intrinsic/off, (III) electron accumulation, and their corresponding band diagrams are

plotted in Figure.3-6. Extrapolation of the linear region results in a  $V_{th} |_{V_{d=1V}}$  of 5.47V. The FET shows an on-current ( $I_{on}$ ) of  $0.47\mu A$ , which is measured at  $V_{GS}=15V$  and  $V_{ds}=1V$ . The curve shows that  $I_{DS}$  decreases exponentially below  $V_{th}$  and  $I_{off}=2.5pA$  when  $V_{GS}=0V$ ,  $V_{DS}=1V$ . The transistor has an on-off current ratio of nearly  $10^5$ . Higher off-state leakage current is observed in NW-TFTs because of the amplification of gate induced drain leakage (GIDL) current by the large area gate to drain overlap, which is deliberately designed for sensing measurement.

The scaling behavior of the NWs FET with respect to channel length  $L$  is shown in Figure 3-7. We can see that the leakage current becomes more severe when the device is shorter than  $1\mu m$ , and  $I_{on} / I_{off}$  ratio is also reduced. The rapid increase of the SS and off-current is attributed to the rapid increase of the direct tunneling current through the entire channel length in the off state as the silicon channel length becomes shorter. The threshold voltage decrease with channel length is listed in Table 3-1.



### **3.3: Engineering of channel doping**

In this work, doping Si-NW is done by ion implant method, and followed by a furnace anneal at  $900^{\circ}C$ , 30 minutes for uniform distribution of the dopant over the channel. Both phosphorous- and boron-doped Si-nanowire channels are created for N



and P type devices, respectively.

Figure 3-8 shows the  $I_D$ - $V_{GS}$  transfer characteristics of a device with nanowire channel length of  $5\mu\text{m}$  with various doping concentrations. The device with higher channel doping depicts lower threshold voltage, higher on-current, albeit degraded SS.

The threshold voltages for devices with different doping concentration are listed in

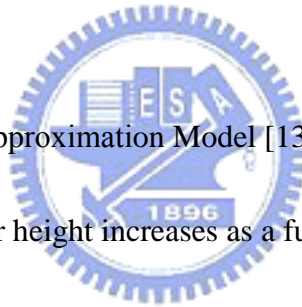
Table 3-2. From Equation 3-6 :  $V_T = V_{FB} + 2\psi_B - (Q_{DM} + qD_I) C_{OX}$ , we derive that

$$\Delta V_T = -qD_I C_{OX}, D_I: \text{dose (cm}^{-2}\text{)}.$$

In the accumulation-mode device with n+n-n+ doping profile, the source-to-drain direct tunneling current is expected to be increased, as there are sufficient carriers in the channel for conduction even at 0V gate bias. Increasing the doping concentration degrades subthreshold swing, while SS is improved in the inversion-mode transistors. This is due to the reduced shielding of the channel region from the drain electric field, resulting in field-enhanced tunneling. The subthreshold current is significantly larger in the accumulation-mode device with higher doping concentration. It appears that devices need to be fully depleted in the off-mode in order to avoid leakage.

In order to improve performance, channel doping is necessary. In TFT device, the height of the barrier is dependent on the defect or trap density at the grain boundary, with a large number of defects resulting in a higher potential barrier. In the

low gate voltage region, the barrier increases with gate voltage because the gate-induced electrons are trapped by the trapping states at the grain boundaries. The barrier height reaches a maximum when the device is in strong inversion. After the trapping levels are fully filled, the barrier height decreases with gate voltage due to the increase of carriers. Potential barrier resulting from grain boundary in the channel acts to suppress current flowing through the channel when the barrier height is greater than the thermal voltage. However, in the device with higher doping channel, as the voltage increases, the dopant ions will fill the grain boundaries, causing a reduction of the potential barrier.



From Seto's Depletion Approximation Model [13]: While the doping density  $N_D < N_T/L_G$ , the potential barrier height increases as a function of  $N_D$ ,  $qV_B = qN_D(L_G^2)/8\epsilon$ , and when  $N_D > N_T/L_G$  the potential barrier height decreases  $qV_B = q(N_T^2)/8\epsilon N_D$ , where  $N_D$  is the doping density,  $N_T$  is the trap density,  $L_G$  is the grain size, and  $\epsilon$  is the dielectric constant of silicon.

We have also investigated the on-current for the accumulation-mode devices with channel length ranging from  $1\mu\text{m}$  to  $10\mu\text{m}$ , and with different channel doping. The results are shown in Figure 3-9. It can be seen that as the channel doping is higher, the on-current increases, especially when  $L$  is shorter than  $1\mu\text{m}$ .

### 3.4: Thin-film-transistor with multiple NW-channels

We present a simple approach based on dummy gate array to create dense and highly ordered poly-silicon nanowire channels. The nanowire space is 1 $\mu$ m.

As shown in Figure 3-10 of a SEM profile, it can be seen that a device consisting of 20 channels is successfully fabricated.

Figure.3-11 shows the improvement in the current driving capability of the multiple-channel FET with 2, 4, 10, and 20 channels. We find improvement of current driving capability for multiple-channel FET with  $L=5\mu\text{m}$ . The drain current ( $I_d$ ) of the multiple-channel FET is found to be multiplied due to the multiple channels in the multiple-channel FET. Assuming that the effective channel width equals the NW diameter ( $d$ ) multiplied by the number ( $N$ ) of NWs,  $W_{\text{eff}} = Nd$ .

Multi-nanowire structure would be a good choice for delivering a strong drive current. The device's key electrical characteristics, such as threshold voltage ( $V_{\text{th}}$ ), and subthreshold swing ( $SS$ ), are also improved by increasing the number of channel.

In nanoscale devices, features such as interfaces, boundaries will play an important role. The density of grain boundary trap states existing in the channel near the pattern edge is much lower than elsewhere. As the channel width is scaled down,

the effect of the poly-Si pattern edge becomes dominant. [14]. The crowding of the gate fringing field at the corner edges is higher than that at other region of the channel. The larger electrical field and better gate control across the corner increase the carrier density. These phenomena are demonstrated by simulation tool-ISE TACD, as shown in Figure 3-12.

Nanowire device will dissipate lower power consumption, so the operation for arrays becomes possible, and multi-functional nanowire sensor could lead to powerful sensor systems.



### **3.5 Effect of O<sub>2</sub> plasma treatment and water environment on device performance**

In the process of integrating PDMS channel into NW-FET, oxygen plasma is used to bind them together. This may adversely affect the device performance. In this section, we report the performance difference for devices with and without oxygen plasma treatment.

Some wafers were subjected to an O<sub>2</sub> plasma treatment system with a pressure of 0.2Torr, RF power of 17W. The duration was 60 sec. Figure 3-13 compares Id-V<sub>GS</sub> characteristics, measured at V<sub>d</sub>=0.1 and 1 V, for Si-NWs TFTs with and without O<sub>2</sub>

plasma treatment. The devices with O<sub>2</sub> plasma treatment show better performance than those without plasma treatment, depicting higher on-current and slightly smaller leakage current and subthreshold swing. It is well known that the subthreshold swing (SS) depends on the ratio of the gate capacitance to other capacitances which are related to the interface trap states, and small SS indicates that the devices have lower interface state after oxygen plasma treatment.

The Si-nanowire channel surface is initially covered by a native oxide, which is known to lead to a high density of states at the silicon-oxide interface and shifts the threshold voltage of a transistor. It is known that O<sub>2</sub> plasma can remove organics, and clean the nanowire surface. Besides, negative charged atom (O<sup>-</sup> and O<sup>2-</sup>) will diffuse through the polysilicon boundaries and passivate surface dangling bonds [15]. The mobility and on-current will be enhanced because oxide and interface charges are critical in allowing the perpendicular electric field to be effectively coupled to the channel and thus affect the channel conductance.

### **3.6 Nanowire surface modification and biotin-streptavidin sensing**

Compared with planar device that binds only to a small region of the surface, the

charged biological or chemical species under accumulation or depletion in the 1D nanowire channel takes place in the “bulk”, thus giving rise to a large change in the electrical properties. As the nanowire diameter decreases, the accumulation/depletion region will occupy greater fraction that potentially enables the detection of what we are most interested in, i.e., small amount molecules level.

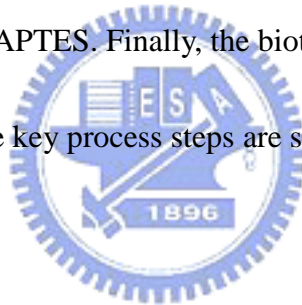
Biochemical sensors usually work in the aqueous sample environment. Before sensing protein, we must know their electrical characteristics. In Figure 3-14, we can see that the device can depict different threshold voltage ( $V_{th}$ ), steeper Swing, and higher subthreshold gate leakage in the water. Because of charged ions, the electrical measurements of nanowire device are complicated by the high background current which can affect the device performance. The high dielectric constant of water also leads to large stray capacitance and better gate control and small SS. Besides, it creates double layer capacitance and low resistance electrolyte. All these factors must be taken into consideration.

We believe that a steeper subthreshold swing can be achieved by using a core-shell structure or using a surrounding gated structure with high-k dielectric.

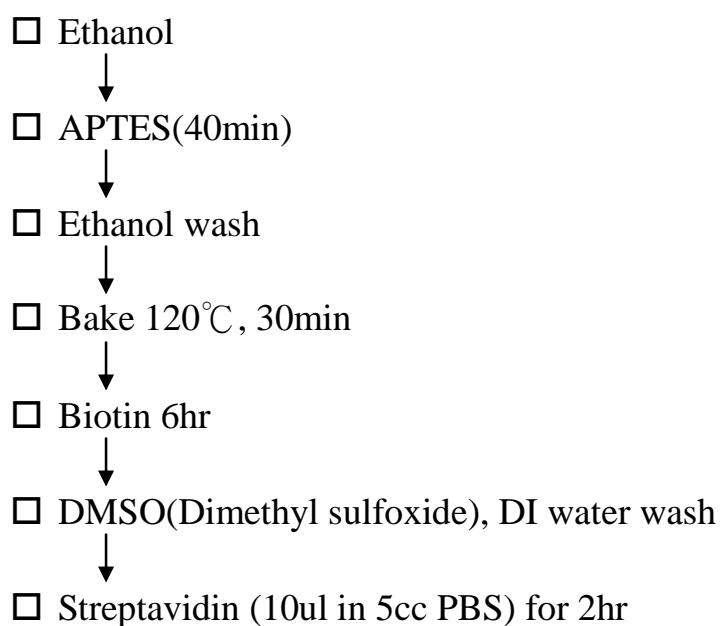
The surface is of extreme importance to the electrical transport and the device performance of semiconductor nanowires. We have investigated how surface modifications of nanowires impact their electrical properties. Briefly, the surface of

Si-NWs must be modified chemically in order to attach biologically active compounds onto Si-NWs before sensing. The oxidized Si-NW surface was then functionalized with a self assembled monolayer aminopropyltriethoxysilane(APTES).The APTES layer changes the surface hydroxyl OH, or silanol SiOH bonds, resulting in an  $-NH_2$  surface termination (Figure 3-15) [16].

After APTES surface was modified, the device was washed with ethanol and baked at  $120^{\circ}C$  for 30min.Then, the device was hold in biotin solution for 6 hours to ensure the biotin linking with APTES. Finally, the biotin was used to capture the streptavidin (Figure 3-16). The key process steps are shown as follows:




Biotin-streptavidin link process flow:



Phosphate buffered saline (PBS)(10mM, pH7.4,140mM NaCl, 3mMKCl) was used in our biological treatment experiment.

From Figure 3-17, measurements are performed on the transistor before treatment, after receptor treatment, and after target treatment. To demonstrate selective bioactivity sensing, devices were functionalized with biotin. The biotin will capture the streptavidin which forms irreversible binds. We have observed that the addition of protein caused a drop in Ion (conductance) and shifted the threshold voltage ( $V_{th}$ ) to the right for the nanowire device. This indicates that the molecules tend to carry negative charges.



Protein has many potential applications due to the functional specificity and broad utility. Proteins can passivate micro device surfaces. We have investigated the binding behavior, structure, and activity of a protein “streptavidin” captured by the biotin on nanowire FET surface. It serves two major purposes: passive coating to reduce adverse foreign responses by the biological system and as functional elements of the device, such that the specific function of the protein is exploited to perform desired diagnostic tasks.



# Chapter 4: Conclusion and Future Work

## 4.1 Conclusion

This thesis presents a method for design, fabrication, and characterization of Si-nanowire TFT integrated with microfluidic channel for nano sensor applications.

We use thin film transistor and sidewall spacer technology to fabricate nanowire TFT without resorting to sophisticated lithography tools. The proposed approach enables the development of multi-channel sensor with well controlled dimension, position, alignment, chemical composition. In addition, the PDMS-based microfluidic device enables an easy and cost effective method to control samples for biomedical sensing.

The electrical properties of NW-TFT, including modified conductivity, adjusted threshold voltage (either with or without phosphorus/boron channel doping), multi-channel, and effects of oxygen plasma have been investigated. Finally, we have described a means of sensing biotin-streptavidin in solution using a compact simple technique that does not rely on tagging or marking instruments.

## 4.2 Future work

The nanowires used in our study were about 40 nm in thickness, which can be made thinner in the future. This will help reduce the tunneling leakage current and sharpen the subthreshold swing for excellent sensitivity. As for the microfluidic channel, the air bubble clogging remains a troublesome problem throughout this study, and needs to be tackled in the future.

The development of nanowire biosensors for the detection of diseases is still in its infancy. However, if we can optimize the system, in a longer perspective, a portable (e.g., in the palm of the hand), remote, flexible [31], implantable (long operational lifetime and biocompatibility) sensor platform will be realized. Moving diagnostics from the clinic to home will not be a fancy dream anymore, and may very well become the standard method of analysis in life sciences in the foreseeable future.



## References:

- [1] Lundstrom, I, Shivaraman, M S ,Svenson, C S ,Lundkvist,” A hydrogen–sensitive MOS field–effect transistor”, Appl Phys Lett ,1975.
- [2] Z. Davis, G. Abadal, O. Kuhn, O. Hansen, F. Grey and A. Boisen, "Fabrication and characterization of nano-resonating devices for mass detection", J. Vac. Sci. Technol. B, Vol. 18(2), 2000.
- [3] Linda S. Jung, Charles T. Campbell, Timothy M. Chinowsky, Mimi N. Mar, and Sinclair S. Yee, “Quantitative Interpretation of the Response of Surface Plasmon Resonance Sensors to Adsorbed Films”, Langmuir ,14, 5636-5648 ,1998.
- [4] P. Bergveld, “Development of an ion-sensitive solid-state device for neurophysiological measurements”, IEEE Transactions on Biomedical Engineering, 1970.
- [5] Yi Cui, Qingqiao Wei, Hongkun Park, Charles M. Lieber,” Nanowire Nanosensors for Highly Sensitive and Selective Detection of Biological and Chemical Species”, Science Vol 293 17, August 2001.
- [6] Patolsky F, Zheng G, Hayden O, Lakadayali M, Zhuang X and Lieber C M, PNAS 101 14017 ,2004.
- [7] Zheng G, Patolsky F, Cui Y, Wang W U and Lieber C M, Nature Biotechnol. 23

1294, 2005.

- [8] H.-C. Lin, M.-H. Lee, C.-J. Su, T.-Y. Huang, C. C. Lee, and Y.-S. Yang, "A Simple and Low-Cost Method to Fabricate TFTs With Poly-Si Nanowire Channel," IEEE Electron Device Letters, Vol. 26, No. 9, September 2005.
- [9] MEMS Exchange, <http://www.mems-exchange.org/>
- [10] H. Sakaki, "Scattering suppression and high-mobility effect of sizequantized electrons in ultrafine semiconductor wire structures," Jpn. J. Appl. Phys., vol. 19, no. 12, pp. L735-L738, 1980.
- [11] Janelle R. Anderson, Daniel T. Chiu,<sup>†</sup> Rebecca J. Jackman, Oksana Cherniavskaya, J. Cooper McDonald, Hongkai Wu, Sue H. Whitesides, and George M. Whitesides, "Fabrication of Topologically Complex Three-Dimensional Microfluidic Systems in PDMS by Rapid Prototyping", Anal. Chem., 72, 3158-3164, 2000.
- [12] Arun Natarajan, Gerko Oskam, and Peter C. Searson, "The Potential Distribution at the Semiconductor/Solution Interface", J. Phys. Chem. B, 102, 7793-7799, 1998
- [13] W Seto, John Y, "The electrical properties of polycrystalline silicon films", Journal of Applied Physics, Volume 46, Issue 12, pp. 5247-5254, 1975.
- [14] Ming-Shan Shieh, Jen-Yi Sang, Chih-Yang Chen, Shen-De Wang and Tan-Fu LEI, "Electrical Characteristics and Reliability of Multi-channel Polycrystalline

Silicon Thin-Film Transistors”, Japanese Journal of Applied Physics Vol. 45,  
No. 4B, 2006.

[15] Horng Nan Chern, Chung Len Lee, Member, ZEEE, and Tan Fu Lei, H<sub>2</sub>/O<sub>2</sub>  
Plasma on Polysilicon Thin-Film Transistor, IEEE Electron Letters, Vol. 14, No.  
3, March 1993

[16] Edwin T. Car, Albert van den Berg, ”Nanowire electrochemical sensors: can we  
live without labels?”, Lab Chip, 7, 19–23, 2007.

[17] D R Bowler, ” Atomic-scale nanowires: physical and electronic  
structure”, J. Phys.: Condens. Matter 16, 2004.

[18] Jing Wang, Eric Polizzi, Avik Ghosh, Supriyo Datta, and Mark Lundstrom, ”  
Theoretical investigation of surface roughness scattering in silicon nanowire  
transistors”, Applied Physics Letters 87, 043101, 2005.

[19] Jing Wang, Eric Polizzi and Mark Lundstrom, ” A Computational Study of  
Ballistic Silicon Nanowire Transistors”, International Electron Devices Meeting,  
2003.

[20] S. Mudanai, G. L. Chindalore, Member W.-K. Shih, H. Wang, Q. Ouyang, Al F.  
Tasch, Jr., Christine M. Maziar, and S. K. Banerjee, “Models for Electron and  
Hole Mobilities in MOS Accumulation Layers”, IEEE Transactions On Electron  
Devices, Vol. 46, No. 8, August 1999.

- [21] A. Terao, D. Flandre, E. Lora-Tamayo, and Fernand Van de Wiele,  
“Measurement of Threshold Voltages of Thin-Film Accumulation-Mode PMOS  
/SOI Transistors”, IEEE Electron Device Letters, Vol. 12. NO. 12, 1991.
- [22] Hans-Oliver Joachim, Yasuo Yamaguchi, Yasuo Inoue, Tadashi Nishimura and  
Natsuro Tsubouchi,” Analytical Modeling of Short-Channel Behavior of  
Accumulation-Mode Transistors on Silicon-on-Insulator Substrate”, Jpn. J. Appl.  
Phys. Vol.33 558-562, 1994.
- [23] Feng Qian, Daem. Kim And Galen H. Kawamoto “Inversion/Accumulation-Mode  
Polysilicon Thin-Film Transistors: Characterization and Unified Modeling” IEEE  
Transactions On Electron Devices, Vol. 35, No. 9, September 1988.
- [24] L.K. Wang, J. Seliskar, T. Bucelot, A. Edenfeld and N. Haddad, “Enhanced  
Performance Of Accumulation Mode 0.5 $\mu$ m CMOS/SOI Operated At 300 K And  
85 K”, International Electron Devices Meeting, Technical Digest, 1991.
- [25] C. A. Dimitriadis and D. H. Tassis, “On the threshold voltage and channel  
conductance of polycrystalline silicon thin-film transistors”, Journal of Applied  
Physics Volume 79, Issue 8, pp. 4431-4437, 1996
- [26] S. N. Rashkeev, D. M. Fleetwood R. D. Schrimpf, and S. T. Pantelides, “Effects

of Hydrogen Motion on Interface Trap Formation and Annealing”, IEEE

Transactions On Nuclear Science, Vol. 51, No. 6, December 2004.

[27 ] Yi Cui, Xiangfeng Duan, Jiangtao Hu, and Charles M. Lieber, ” Doping and Electrical Transport in Silicon Nanowires”, Journal of Physical Chemistry B Volume 104, Number 22, June 8, 2000.

[28] R. Venugopal, M. Paulsson, S. Goasguen, S. Datta, and M. S. Lundstrom, “A simple quantum mechanical treatment of scattering in nanoscale transistors”, Journal Of Applied Physics Volume 93, Number 9, 2003.

[29] B. Ashcroftl, B. Takulapalli, J. Yang, G. M. Laws, H. Q. Zhang, N. J. Tao,S. Lindsay, D. Gust, and T. J. Thornton,,” Calibration of a pH sensitive buried channel silicon-on-insulator MOSFET for sensor applications” , Phys. Stat. Sol. (b) 241, No. 10, 2291–2296 ,2004.

[30] E. Stern, G. Cheng, M. P. Young, and M. A. Reed,” Specific contact resistivity of nanowire devices”, Applied Physics Letters, 2006.

[31] W. M. Weber, A. P. Graham, G. S. Duesberg, M. Liebau, C. Cheze and L. Geelhaar, E. Unger, W. Pamler, W. Hoenlein, H. Riechert and F. Kreupl, P. Lugli, “Non-Linear Gate Length Dependence of On-Current in Si-Nanowire FETs”, Solid-State Device Research Conference, 2006.

[32] Deniz Armani, Chang Liu and Narayan Aluru, “RE-Configurable Fluid Circuits By PDMS Elastomer Micromachining”, MEMS '99. Twelfth IEEE International Conference on, 1999.

[33] S J Tan, I K Lao, H M Ji, A Agarwal, N Balasubramanian and D L Kwong, “ Microfluidic design for bio-sample delivery to silicon nanowire biosensor – a simulation study”, Journal of Physics: Conference Series 34 626–630,2006.

[34] A. Alec Talin, Luke L. Hunter, François Léonard, and Bhavin Rokad,” Large area, dense silicon nanowire array chemical sensors”, Applied Physics Letters 89, 153102 ,2006.

[35] Michael C. Mcalpine, Habib Ahmad, Dunwei Wang And James R. Heath,” Highly ordered nanowire arrays on plastic substrates for ultrasensitive flexible chemical sensors”, nature materials Vol 6 May 2007.

[36] H.Watakabe, T.Sameshima,” Oxygen plasma and high pressure H<sub>2</sub>O vapor heat treatments used to fabricate polycrystalline silicon thin film transistors”, Appl. Phys. A 77, 141–144, 2003.

[37] Jim Kling,” Moving diagnostics from the bench to the bedside”, Nature Biotechnology, 2006.

[38] A. Vaseashta, J. Irudayaraj, “Nanostructured And Nanoscale Devices And Sensors”, Journal of Optoelectronics and Advanced Materials Vol. 7, No. 1,

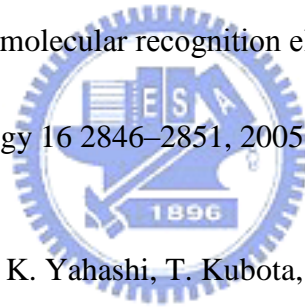


February 2005.

[39] Joseph R. Stetter, Peter J. Hesketh, and Gary W. Hunter,” Sensors: Engineering Structures and Materials from Micro to Nano”, The Electrochemical Society Interface, Spring 2006.

[40] J. Justin Gooding, “Nanoscale Biosensors: Significant Advantages over Larger Devices”, journal of small , Volume 2, Issue 3, Pages 313 – 315, 2006.

[41] Lu Shang, Tami Lasseter Clare, Mark A Eriksson, Matthew S Marcus, Kevin Metz and Robert J Hamers,” Electrical characterization of nanowire bridges incorporating biomolecular recognition elements”, Institute Of Physics Publishing Nanotechnology 16 2846–2851, 2005.



[42] A. Kaneko, A. Yagishita, K. Yahashi, T. Kubota, M. Omura, K. Matsuo, I. Mizushima, K. Okano, H. Kawasaki, S. Inaba, T. Izumida, T. Kanemura, N. Aoki, K. Ishimaru, H. Ishiuchi, K. Suguro, K. Eguchi, Y. Tsunashima,” Sidewall Transfer Process and Selective Gate Sidewall Spacer Formation Technology for Sub-15nm FinFET with Elevated Source/Drain Extension”, International Electron Devices Meeting IEDM Technical Digest. IEEE International, 2005.

[43] Abhisek Dixit, Anil Kottantharayil, Member, Nadine Collaert, Mike Goodwin, Malgorzata Jurczak, and Kristin De Meyer,” Analysis of the Parasitic S/D

Resistance in Multiple-Gate FETs”, IEEE Transactions On Electron Devices, Vol. 52, NO. 6, JUNE 2005.

[44] Michael A. Strosio, And Mitra Dutta,” Integrated Biological-Semiconductor Devices”, Proceedings Of The IEEE, Vol. 93, No. 10, October, 2005.

[45] Sung Dae Suk, Sung-Young Lee, Sung-Min Kim, Eun-Jung Yoon, Min-Sang Kim, Ming Li, Chang Woo Oh, Kyoung Hwan Yeo, Sung Hwan Kim, Dong-Suk Shin, Kwan-Heum Lee, Heung Sik Park, Jeong Nam Han, C.J. Park, Jong-Bong Park, Dong-Won Kim, Donggun Park and Byung-Il Ryu,” High Performance 5nm radius Twin Silicon Nanowire MOSFET (TSNWFET) :Fabrication on Bulk Si Wafer, Characteristics, and Reliability”, International Electron Devices Meeting, IEDM Technical Digest. IEEE International, 2005.



[46] Xiangfeng Duan, Chunming Niu, Vijendra Sahi, Jian Chen, J. Wallace Parce, Stephen Empeocles & Jay L. Goldman,” High-performance thin-film transistors using semiconductor nanowires and nanoribbons”, Nature Vol 425 18 September, 2003.

[47] Todd Thorsen, Sebastian J. Maerkl, Stephen R. Quake, “Microfluidic Large-Scale Integration”, Science 298, 580 ,2002.

[48] A. Valletta, L. Mariucci, A. Bonfiglietti, G. Fortunato, S.D. Brotherton,” Channel doping effects in poly-Si thin film transistors”, Thin Solid Films 487, 2005.

[49] C. T. Black, "Self-aligned self assembly of multi-nanowire silicon field effect transistors", Applied Physics Letters, 2005.

[50] Slides by Prof. Supriyo Datta, Purdue University, 2003.

[51] Slides by Prof. Mark Lundstrom, Electrical and Computer Engineering, Purdue University, 2006.

[52] Slides by James F. Leary, Professor of Basic Medical Sciences and Biomedical Engineering Purdue University, 2006.

[53] Slides by Dr. Hang Lu, MIT.

[54] Links: <http://www.nanohub.org/>

(Nanodevice online simulation and research supported by Purdue University)



	Our approach	VLS	SOI
Small	○	○	○
Rapid real time response	○	○	○
Selectivity	○	○	○
Quantitative	○	○	○
Sensitive	△	○	○
Reproducible(commercialize)	○	X	△
Multifunction	○	○	○
Robustness & Stability	○	X	○
low cost	○	△	X

Table.1-1: Comparisons of the advantage to other current researches

1. Bio & chemical compatibility (its surface properties help prevent cellular materials from adhering)
2. Easy to fabricate
3. Soft
4. pervious to light (within the visible spectrum, therefore easy to monitor the fluid flow and determine the functional integrity of fluidic circuits)
5. Cheaper

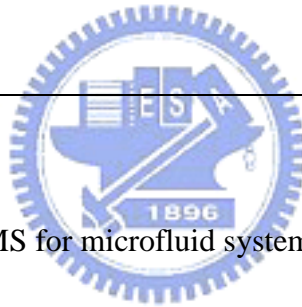


Table. 2-1: advantages of PDMS for microfluid system

	Si	SiO <sub>2</sub>	PDMS
0(s)	135.0	30.33	104.98
30(s)	3.72	7.74	4.27
60(s)	2.17	2.19	2.89

Table.2-2: Θ vs. oxygen plasma time

	L=1μm	L=5μm	L=10μm
N	2.17(v)	5.06(v)	5.30(v)
P	-3.39(v)	-3.74(v)	-4.2(v)

Table.3-1: threshold voltage for different channel length FET

	1E14(cm <sup>-2</sup> )	5E13(cm <sup>-2</sup> )	1E13(cm <sup>-2</sup> )	0(cm <sup>-2</sup> )
V <sub>th</sub> (V)	4.68	5.52	6.26	6.29

Table.3-2: threshold voltage for different channel doping concentration

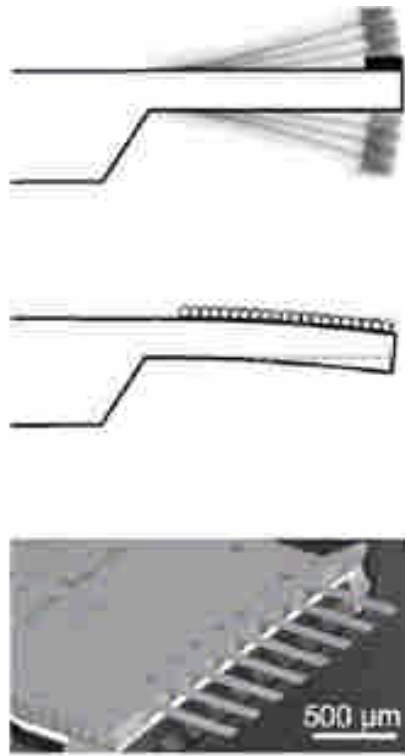


Figure.1-1 Nano cantilevers: absorption of analyte molecules leads to a shift in resonance frequency. [Z. Davis, G. Abadal, O. Kuhn, O. Hansen, F. Grey and A. Boisen]

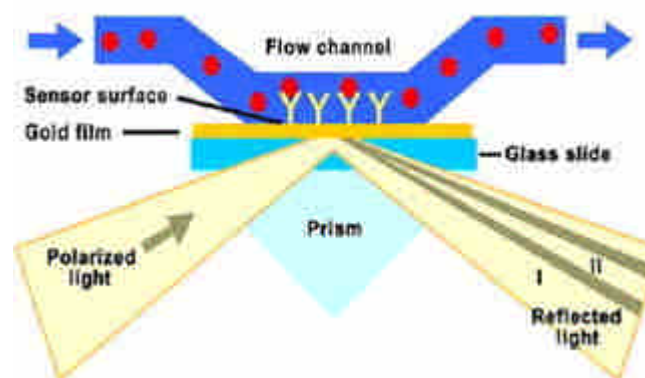
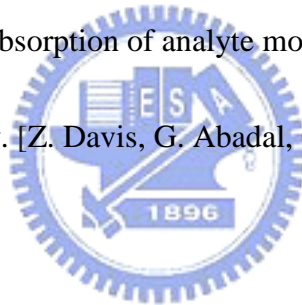


Figure.1-2 Basic components of an instrument for SPR biosensing: a variation in reflectivity of the incident light versus angle or wavelength is proportional to the amount of biopolymer bound near the surface. [Charles T. Campbell]

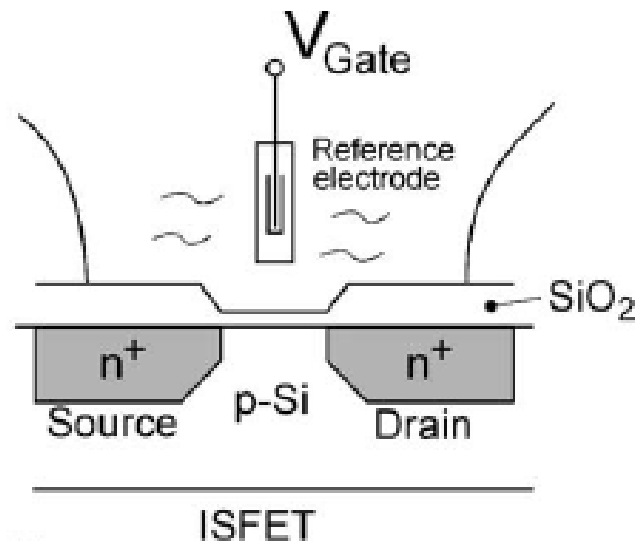


Figure.1-3 Sensing operation of ISFET: the amount of charge of the target species

bound to the surface determines the drain current of the device. [P. Bergveld]

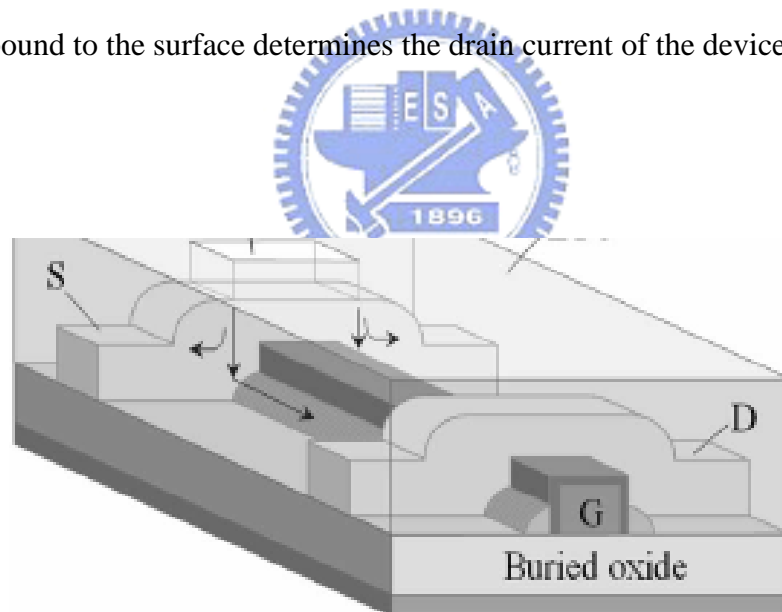


Figure.1-4: FET with nanowires channels proposed by ADTL lab, NCTU



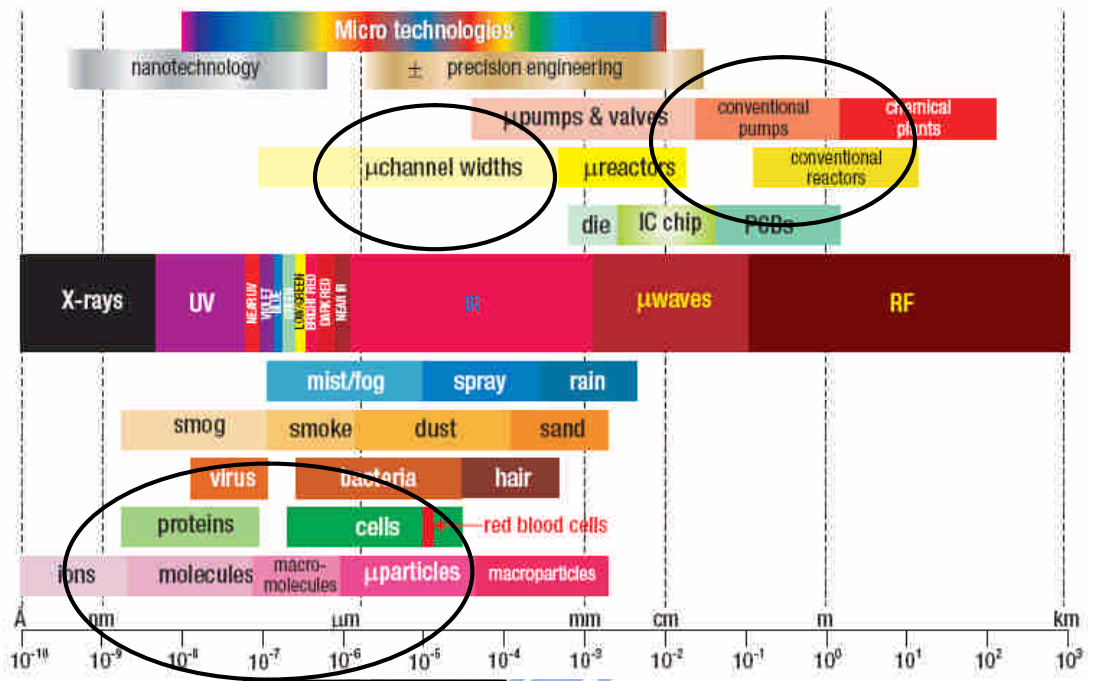


Figure.2-1: Size comparison of various engineering and biological components.  
 [Adapted from A. van den Berg]

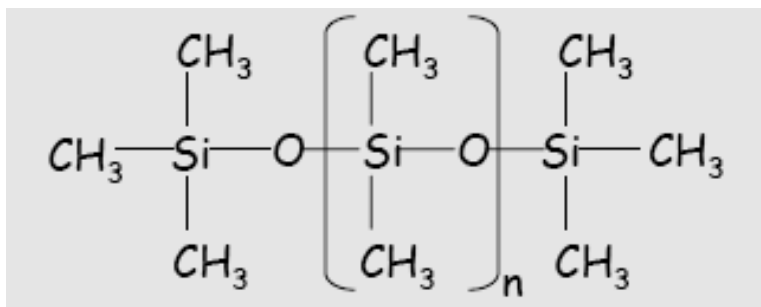


Figure.2-2: structural formula of PDMS

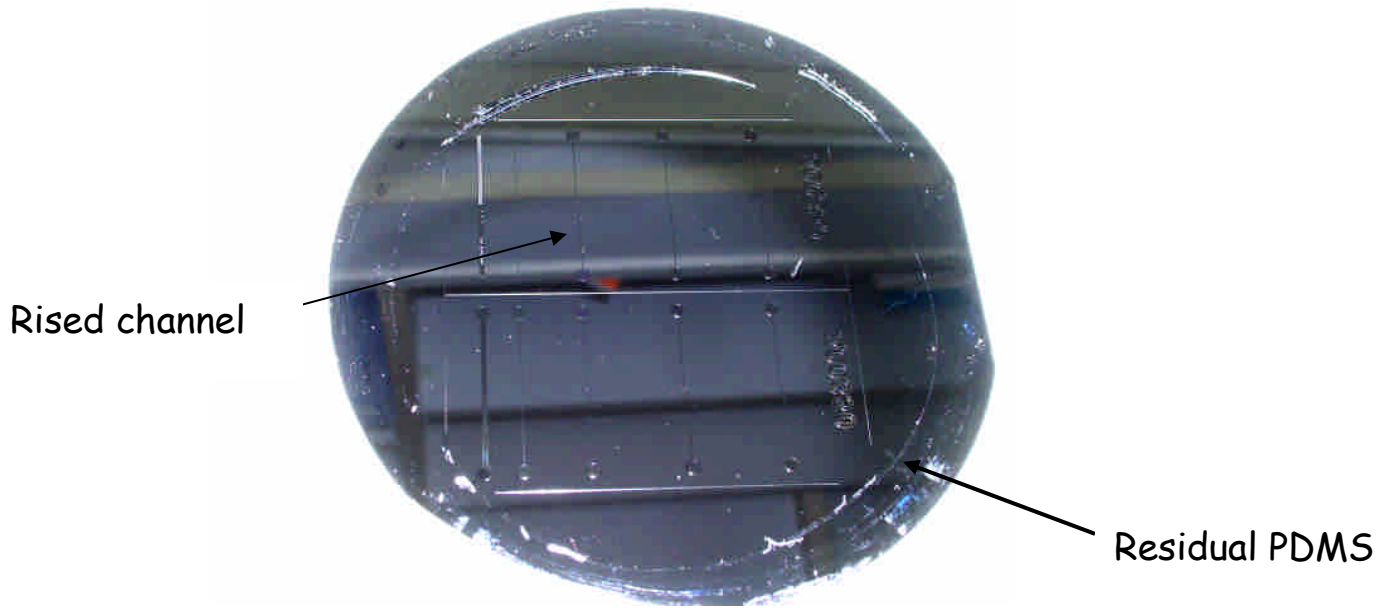


Figure.2-3: SU8 patterns on 4" wafer, Channel length: 3cm; width: 500, 800um; height of resist thickness is about 50um

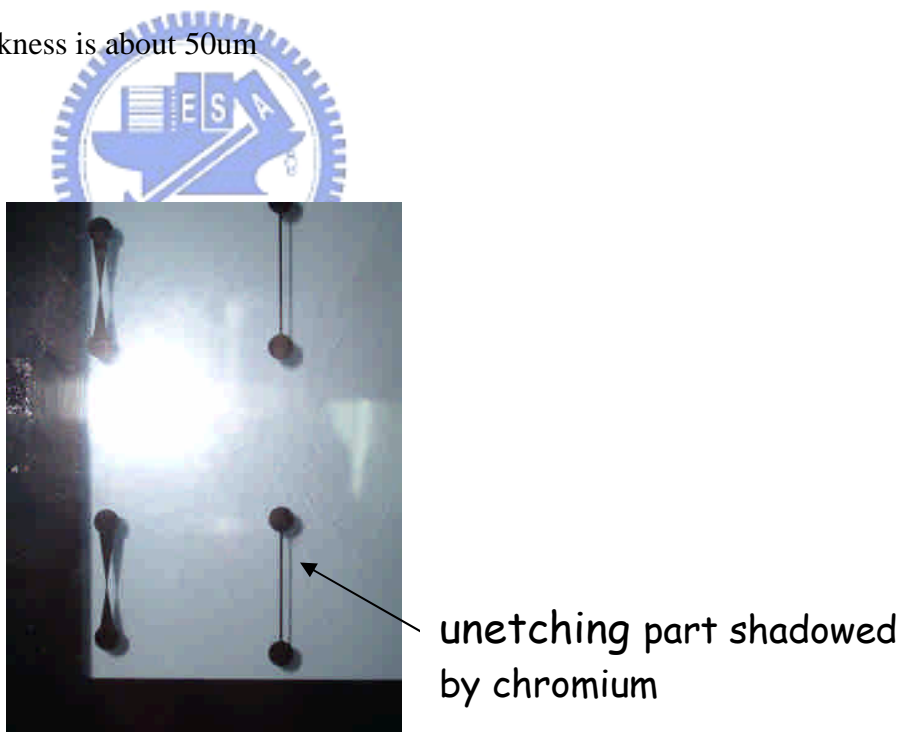


Figure.2-4: different design patterns of microfluidics with glass mask

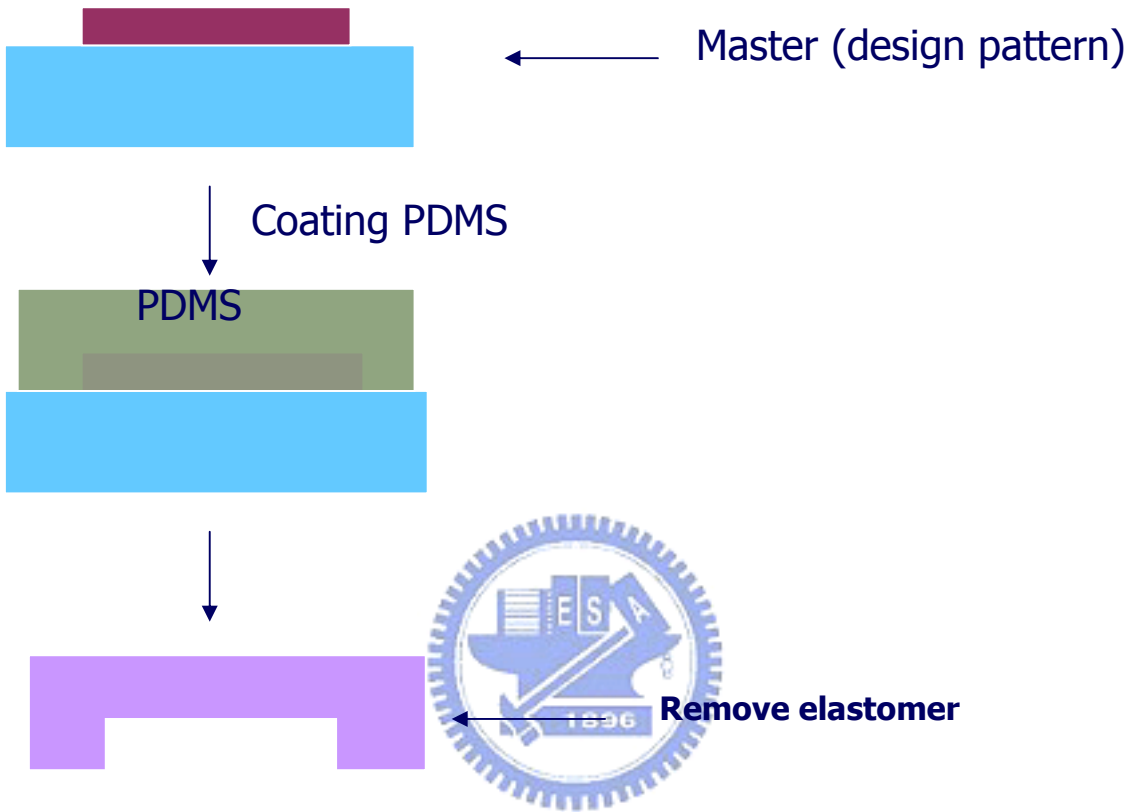


Figure.2-5: cycle of PDMS microfluidic channel



Figure.2-6: finished products with in/out tubes



Figure.2-7: O<sub>2</sub> plasma treatment chamber

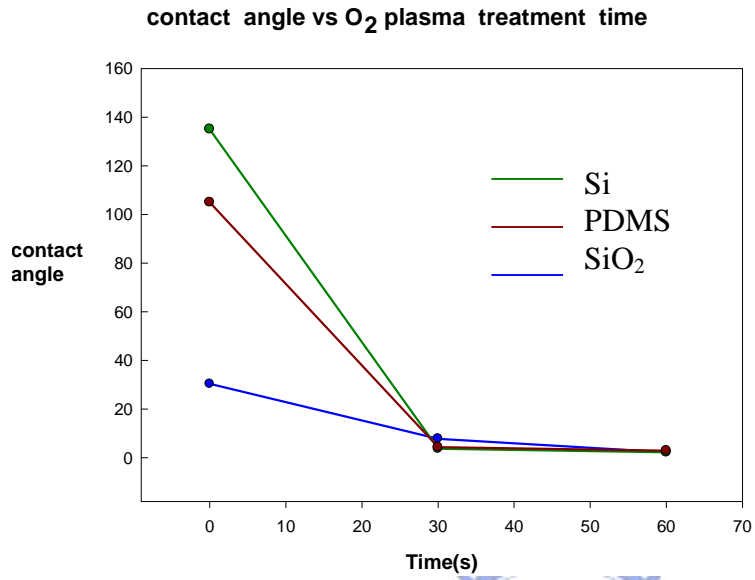


Figure.2-8: contact angle ( $\Theta$ ) of three materials with O<sub>2</sub> plasma treatment time

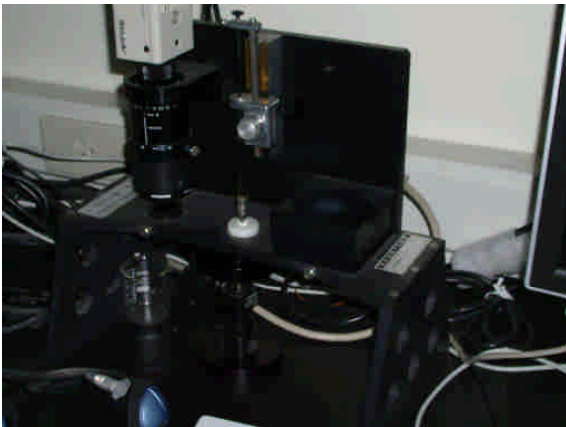


Figure.2-9: contact angle measurement system

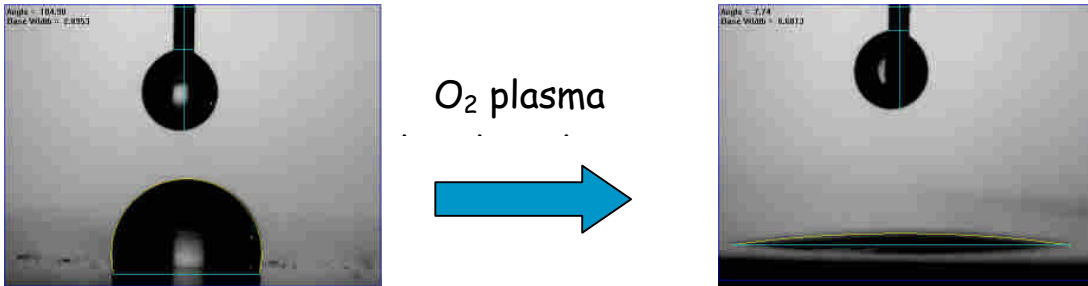


Figure.2-10: surface state of water drop



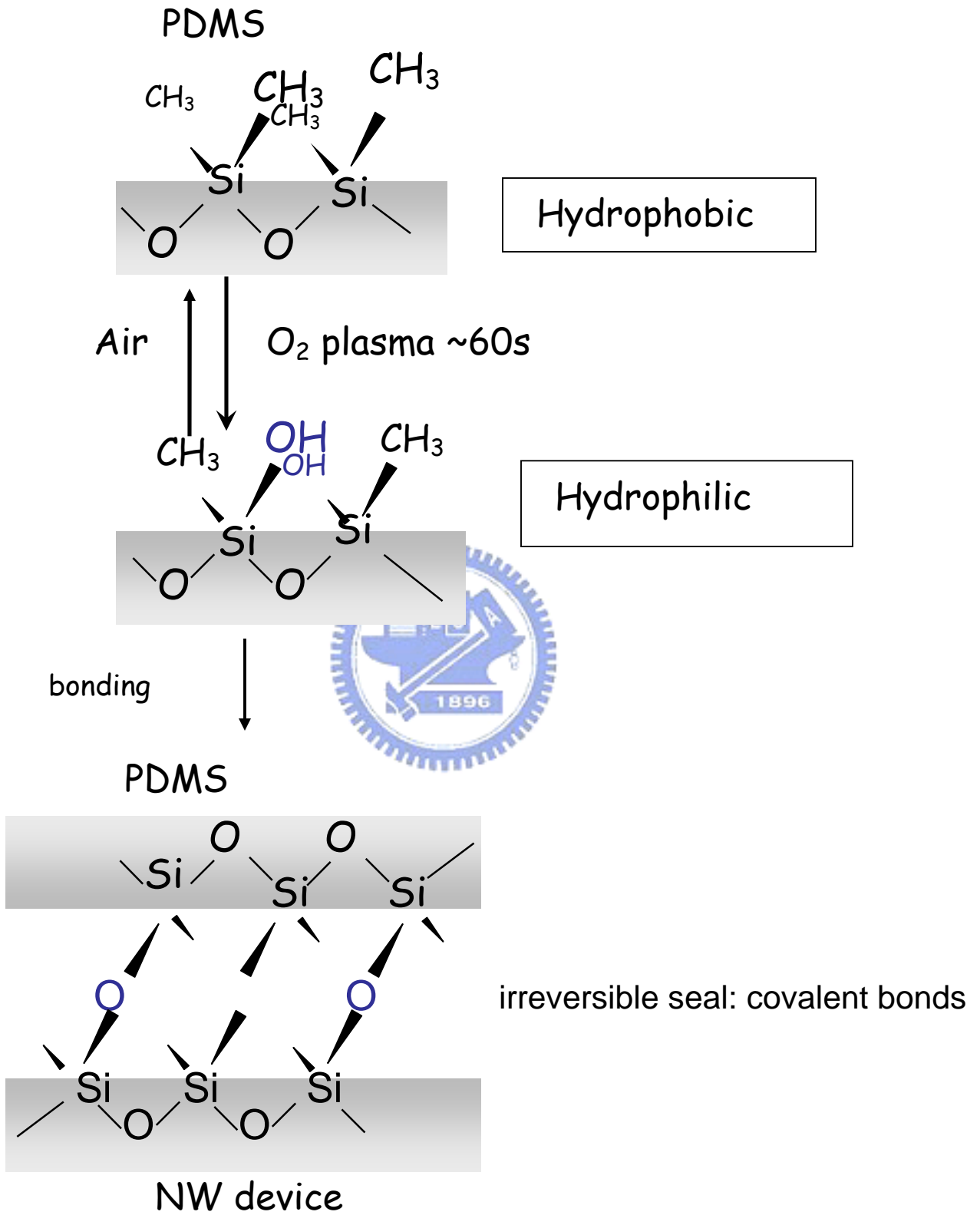


Figure.2-11: Combining process of PDMS and nanowire device



Figure.2-12: controllable syringe pump

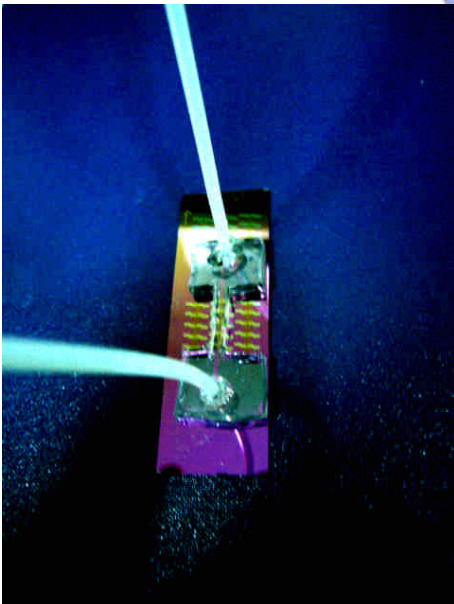
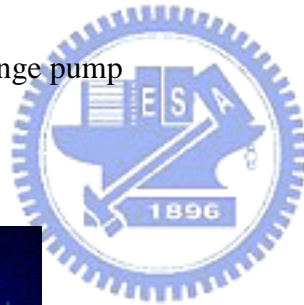


Figure.2-13: NWs TFT integrated with microfluidic system



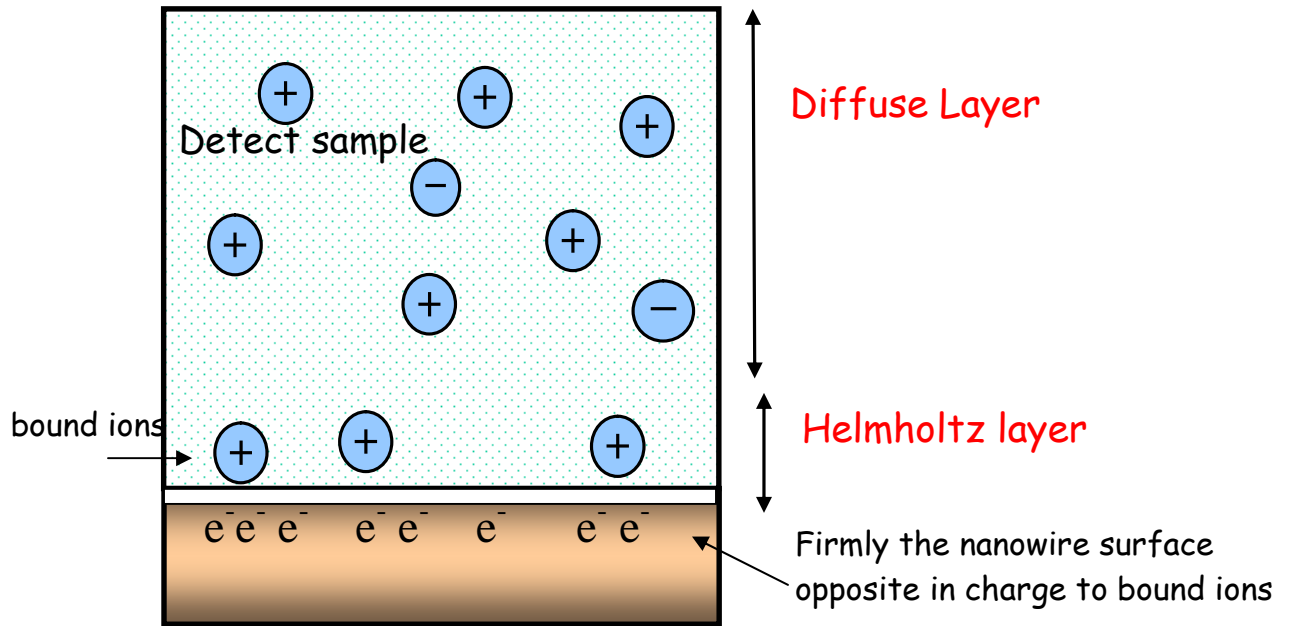


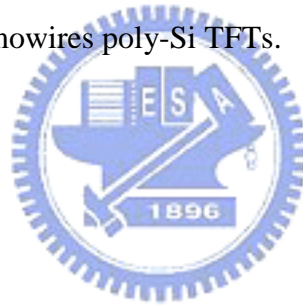
Figure.2-14: liquid and nanowire interface



**NWs-FET fabrication process flow:**

- Deposition wet oxide (1000Å) as gate oxide-(a)
- Dummy gate pattern (TEOS 1000 Å) formation-(b)
- Amorphous-Si deposition and ion implant channel doping-(c)
- SPC: 600°C 24hr
- Nanowires etching by sidewall process and self aligned S/D formation-(d)
- S/D implantation & activation
- passivation and pad formation

Figure.3-1. Process flow of nanowires poly-Si TFTs.



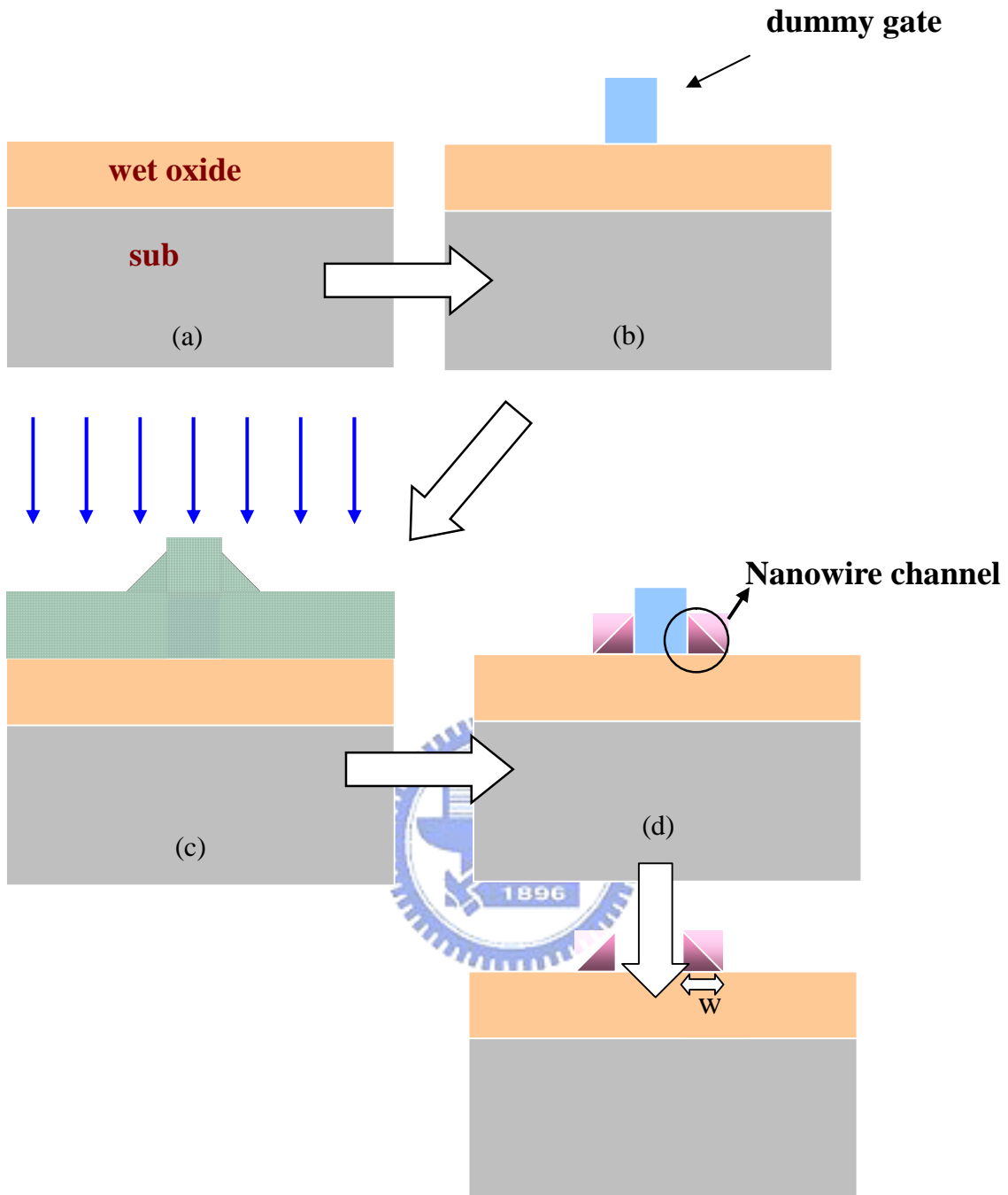


Figure.3-2: Schematic diagram of sidewall twin Nanowires FET process

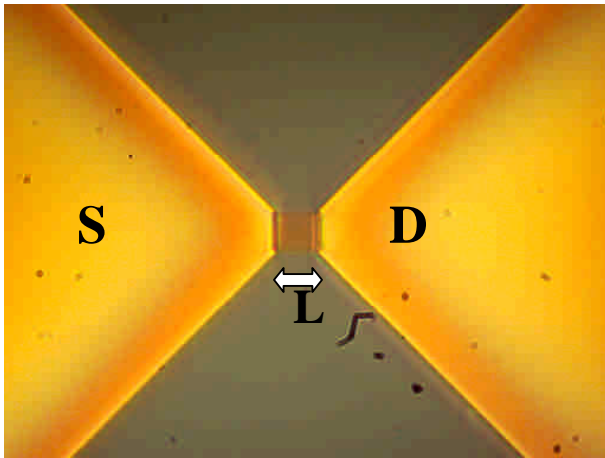


Figure.3-3: Optical microscope image of NWs FET device

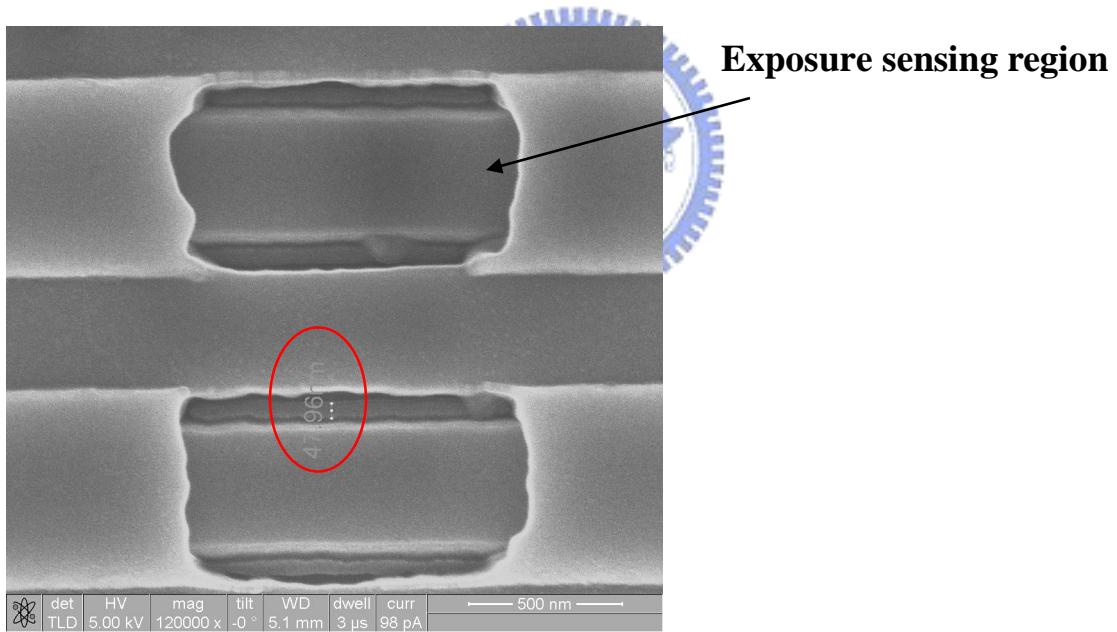


Figure.3-4: SEM graph of sidewall twin nanowires with 47 nm channel width

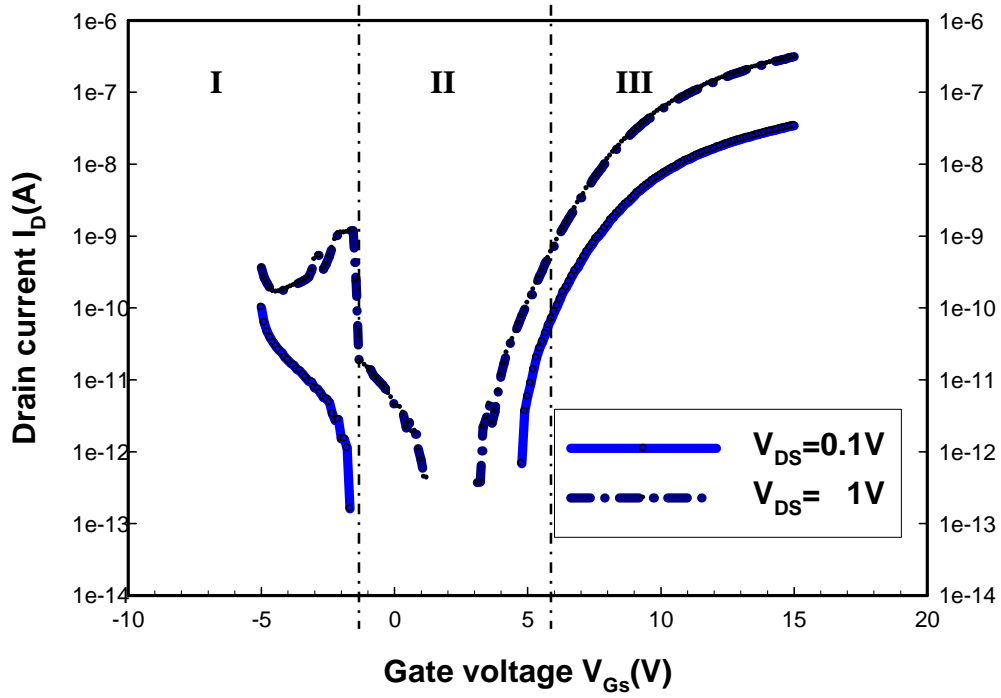


Figure.3-5:  $I_D$ - $V_{GS}$  transfer characteristics of channel doping  $P_{31+}$  with  $5\mu m$  channel length

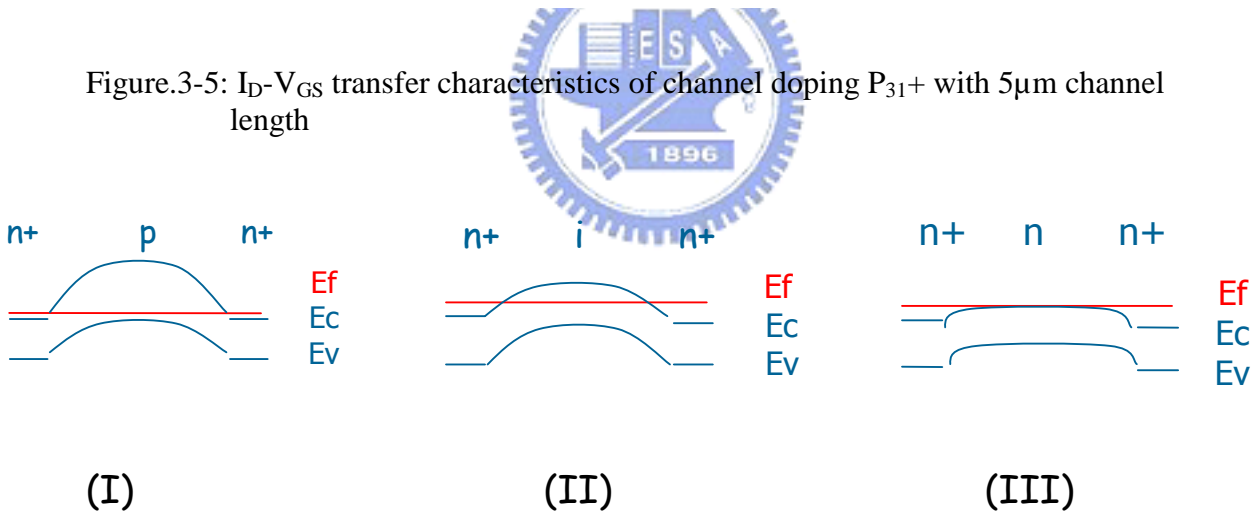


Figure.3-6: Band diagrams of different gate voltage conditions from depletion (I) to accumulation (III) for N-type device

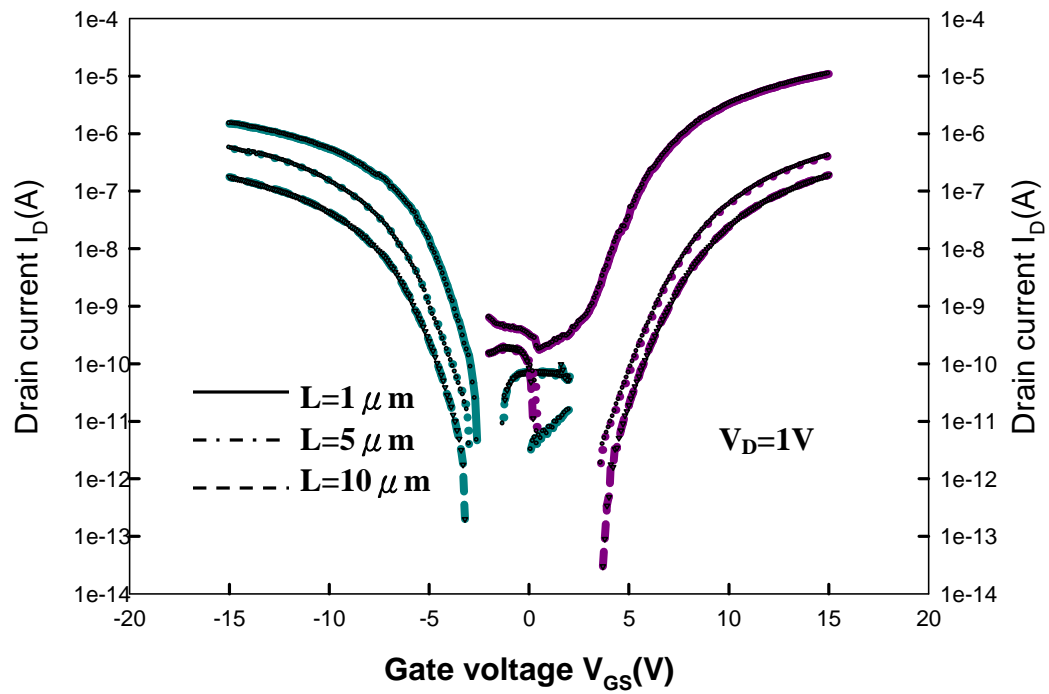


Figure.3-7: transfer characteristics of N/P type NWs-TFT with different channel length



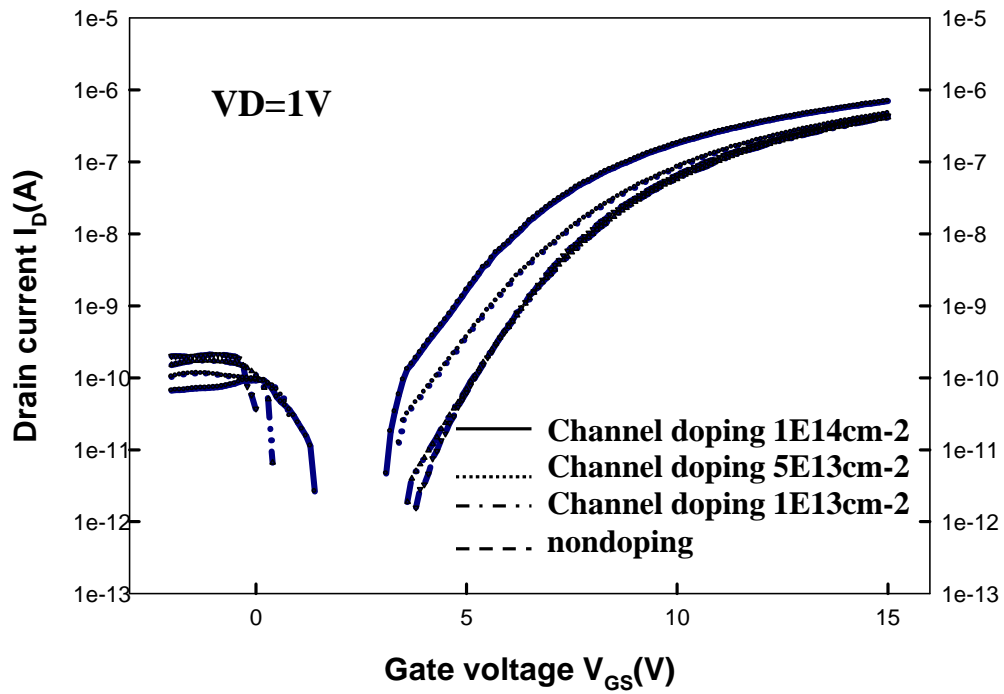


Figure.3-8:  $I_D$ - $V_{GS}$  transfer characteristics of  $5 \mu\text{m}$  channel length device with different doping concentration

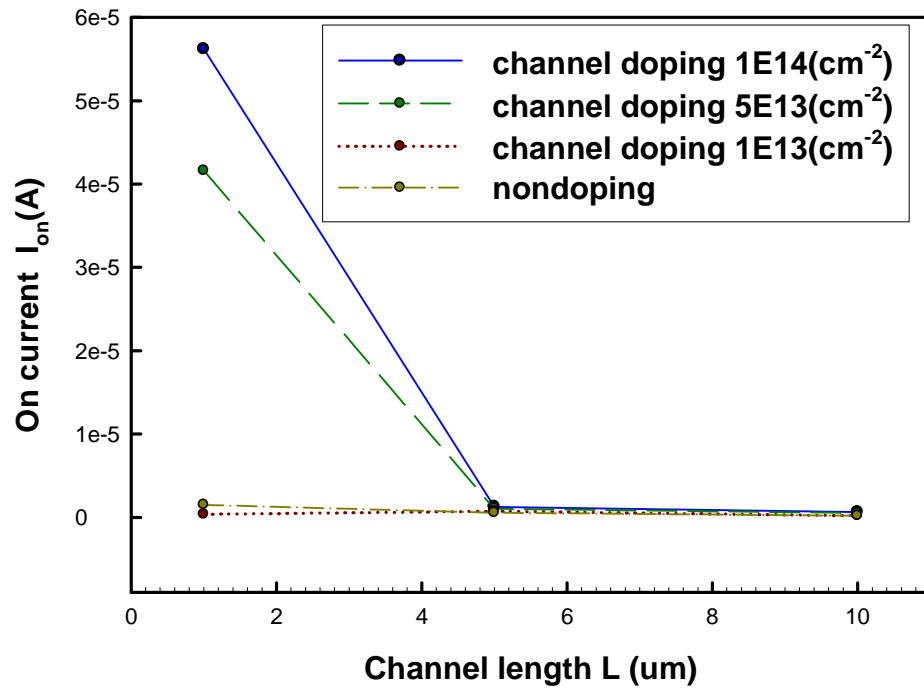


Figure.3-9 : Plot shows the increase of on-current with decreasing channel length for different channel doping level.

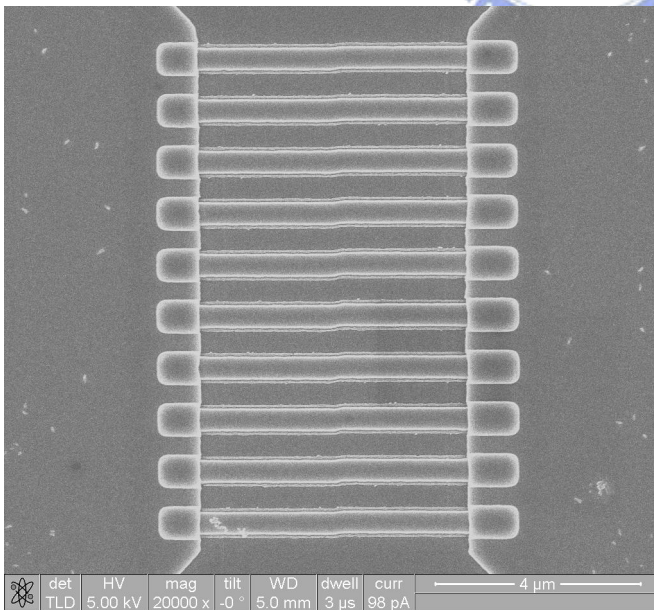


Figure3-10: SEM top view picture of 20 multi parallel nanowires channel TFT width  $W \sim 40$  nm; channel length  $L = 5$   $\mu$ m.



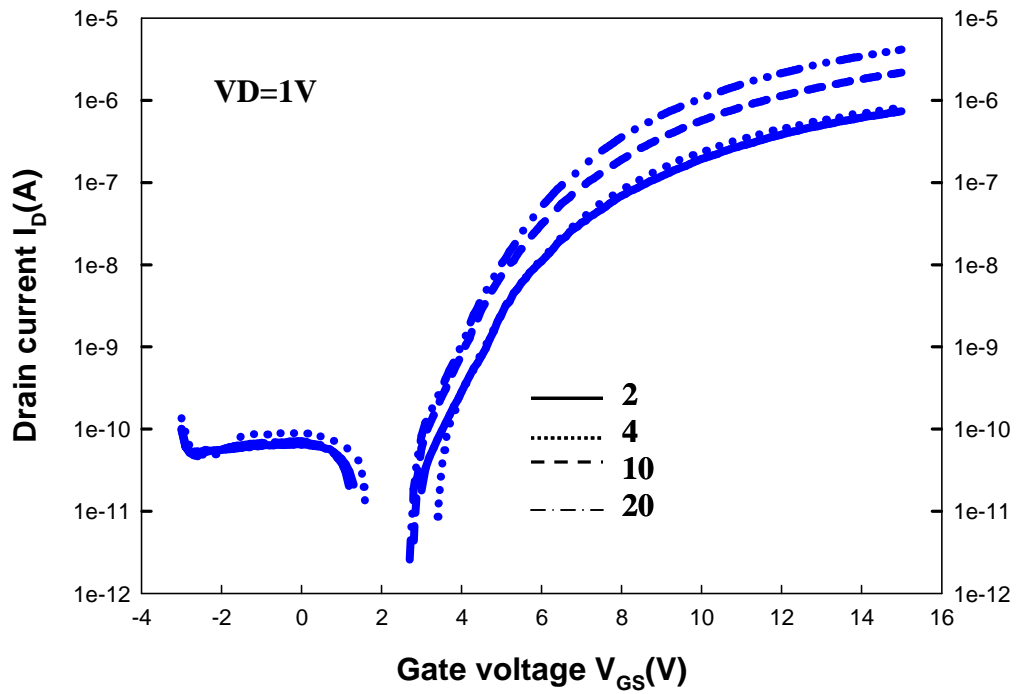


Figure.3-11: Transfer characteristics of NWs-TFT with different channel number

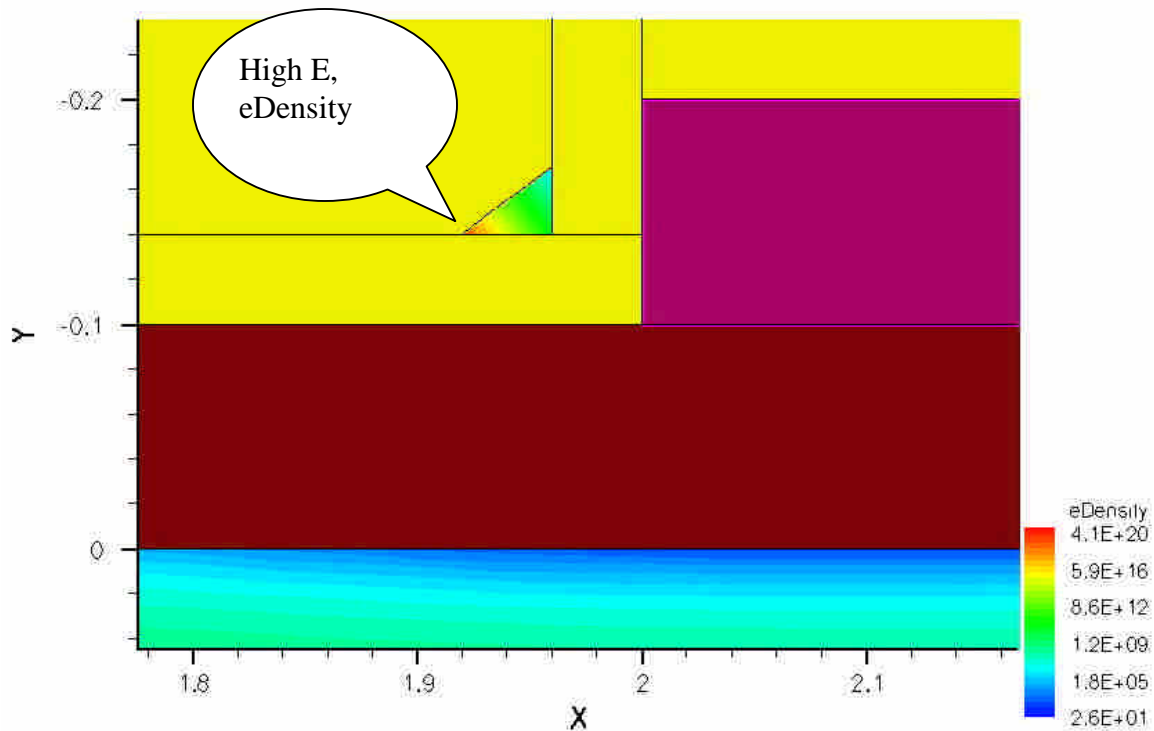


Figure.3-12: ISE-TCAD simulation with bottom gate 5V

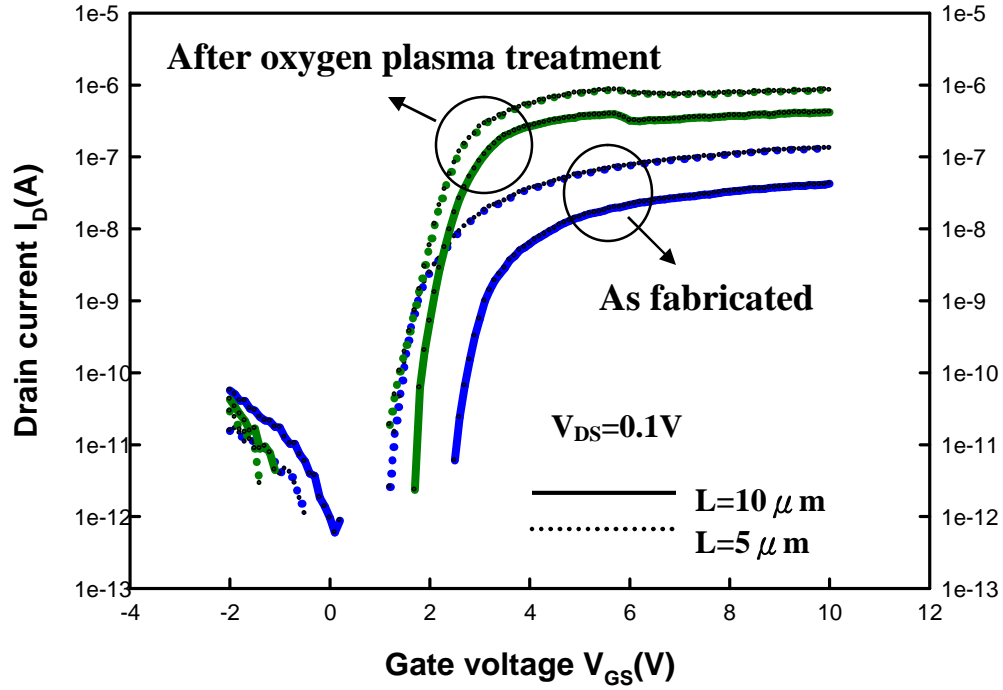


Figure.3-13: The  $I_D$ - $V_{GS}$  characteristics of different length NWs-TFT with/without oxygen plasma treatment.

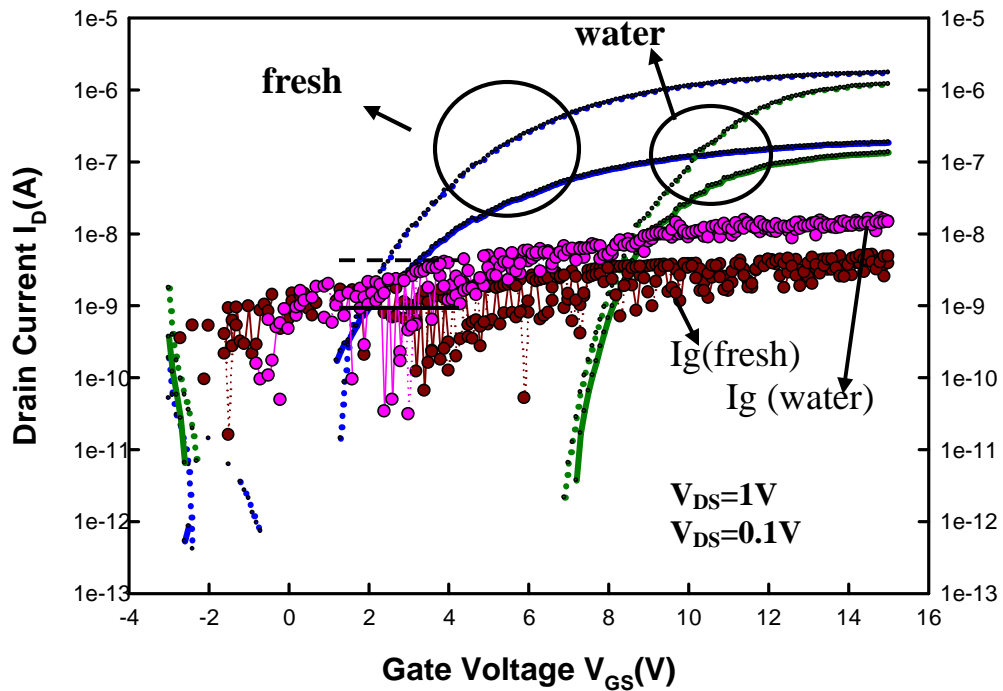


Figure.3-14: Transfer characteristic of device working in the air and water.

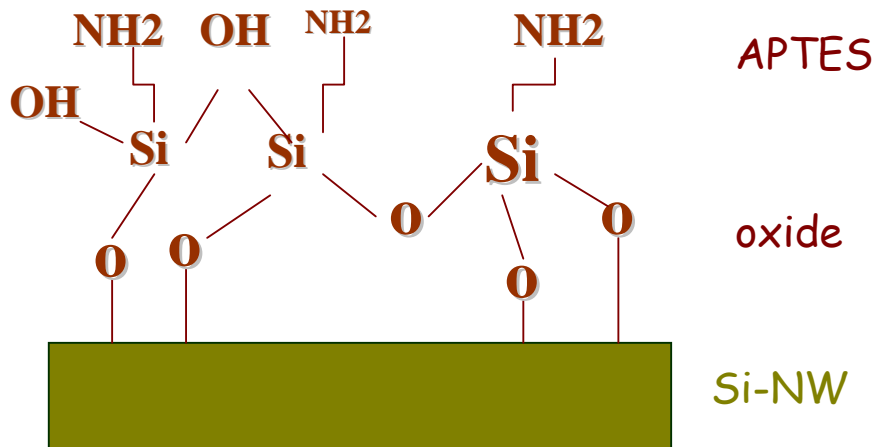


Figure.3-15: Surface bonds of APTES-modified nanowire channel.

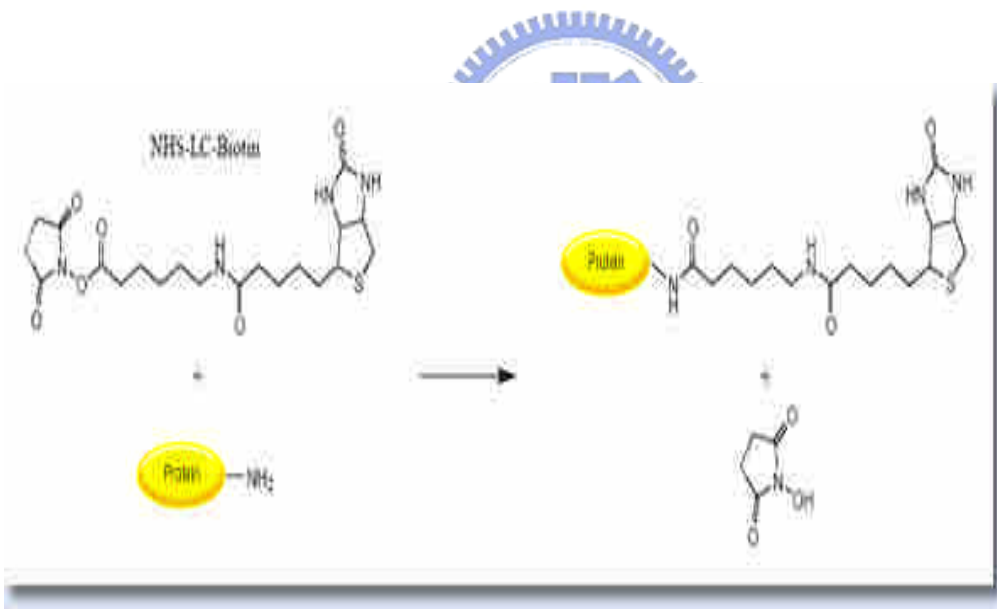


Figure.3-16: Reaction of NHS -Biotin with a primary amine.  
(source: Avidin-Biotin Chemistry: A Handbook)

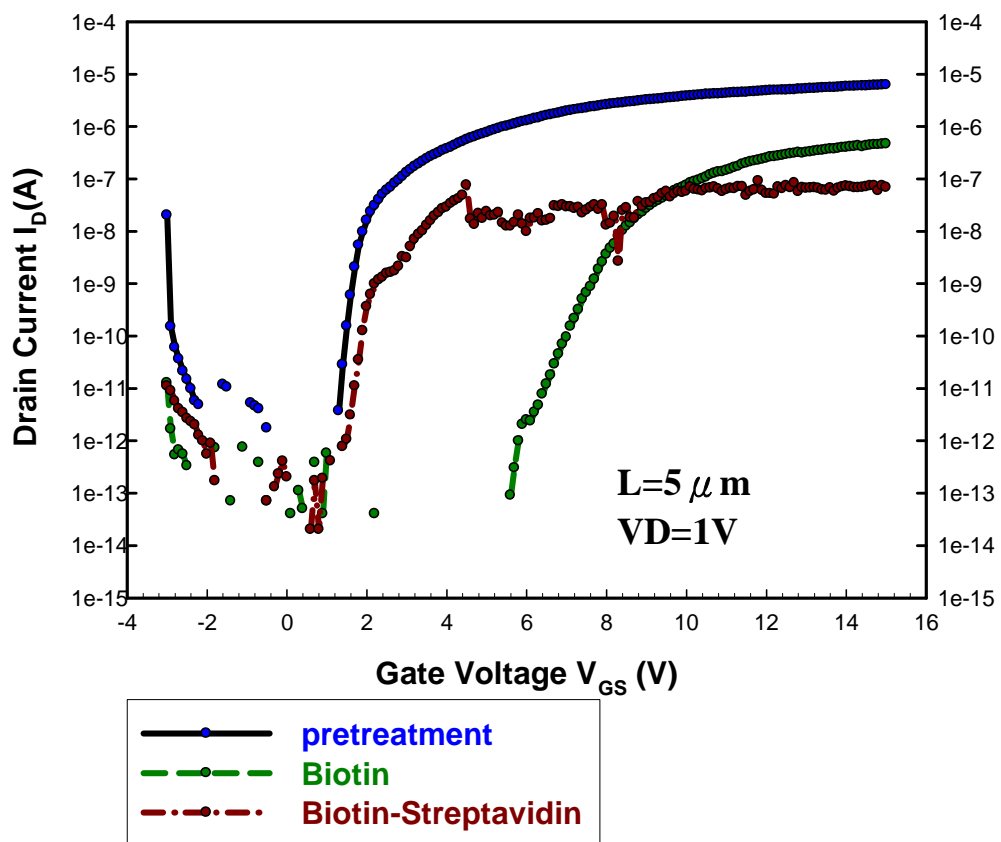
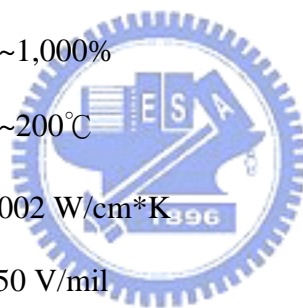


Figure.3-17: Transfer characteristics of NWs-TFT before and after Biotin linking, and sensing of Biotin-Streptavidin.

## APPENDIX

### PDMS property:

mixed viscosity	60,000 cps
hardness	Shore A24
tensile strength	500 psi(Young's modulus 0.5 MPa)
tear strength	125 lb/in
tensile elongation	10~1,000%
temperature range	-55~200°C
thermal conductivity	0.002 W/cm*K
dielectric strength	550 V/mil
(volume resistivity)	1.6*E15 Ω*cm



after solidified, can resist : DHF 、 alcohol 、 short time oxygen plasma erosion

Not sustain long time in ace, base solution

Penetrable by chemical vapor

source : Instrument Technology Research Center

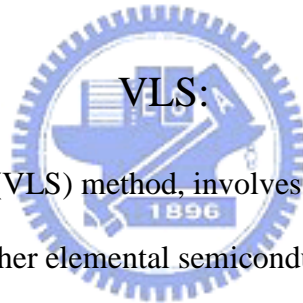
## Nanowire:

1500's: 1-D crystal growth

(whisker) found in ore.

1970's: 1-D "microwire" synthesized.

1990's: 1-D "nanowire" made possible by nanoscale fabrication and characterization techniques.



### VLS:

The vapor – liquid – solid (VLS) method, involves the use of liquid –metal solvents with low solubility for Si and other elemental semiconductor materials. This method has been very successful in producing SiNWs in large quantities and at low temperatures.

The vapor – liquid – solid (VLS) method is the most successful in generating large quantities of nanowires with single crystalline structures. Originally developed in 1964 for single crystals growth the VLS method has since been used to synthesize various inorganic nanowires and nanorods. In this VLS process, a metal, such as gold, that forms a low temperature eutectic phase with silicon is used as the catalyst for nanowire growth. A Si gas source (silane or silicon tetrachloride) is passed over the metal catalyst, which is heated to a temperature greater than the eutectic temperature. The Si gas source decomposes on the surface of the catalyst, and Si diffuses into the metal, forming an alloy. Upon reaching super saturation, SiNWs are precipitated and the liquid alloy drop remains

on the nanowire as it grows in length. The diameter of the SiNWs is controlled by the initial size of the metal catalyst and, to some extent, the growth conditions. Porous alumina membranes have recently been used as an alternative to control nanowire diameter in the VLS process. Defect-free SiNWs with diameters in the range of several microns were synthesized using a supercritical fluid solution-phase approach wherein alkanethiol-coated Au nanocrystals (2.5 nm in diameter) were used as seeds to direct the one-dimensional crystallization of Si in a solvent heated and pressurized above its critical point.

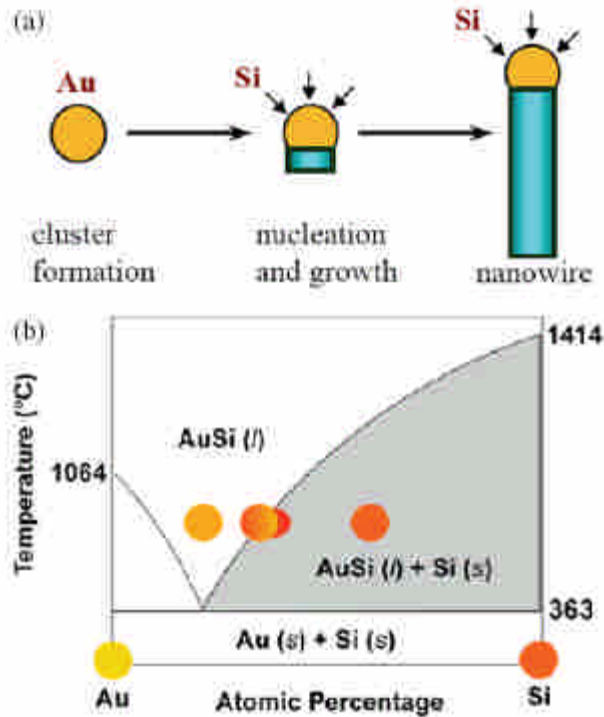


**Figure 1.** Schematic of VLS growth of Si nanowires (SiNWs). (a) A liquid alloy droplet AuSi is first formed above the eutectic temperature (363 °C) of Au and Si. The continued feeding of Si in the vapour phase into the liquid alloy causes oversaturation of the liquid alloy, resulting in nucleation and directional nanowire growth. (b) Binary phase diagram for Au and Si illustrating the thermodynamics of VLS growth.

[Wei Lu and Charles M Lieber]

## Vita

姓名：王子銘 Tzu Ming Wang

性別：男

生日：西元1982年6月15日

出生地：高雄縣

學歷：

國立鳳山高中..... 1997. 09~2000. 06

國立交通大學機械系..... 2001. 09~2005. 06

國立交通大學電子所..... 2005. 09~2007. 06

論文題目：奈米線薄膜電晶體於生化感測應用之研究

Study of Nanowires Thin-Film-Transistor for  
Biochemical Sensor applications